COMPLEXITY NEAR CRITICAL POINTS

by

Uday Sood

A Dissertation

Submitted to the Faculty of Purdue University

In Partial Fulfillment of the Requirements for the degree of

Doctor of Philosophy

Department of Physics and Astronomy

West Lafayette, Indiana

December 2023

THE PURDUE UNIVERSITY GRADUATE SCHOOL
STATEMENT OF COMMITTEE APPROVAL

Dr. Martin Kruczenski, Chair

Dept. of Physics and Astronomy

Dr. Chen-Lung Hung

Dept. of Physics and Astronomy

Dr. Sergei Khlebnikov

Dept. of Physics and Astronomy

Dr. Nima Lashkari

Dept. of Physics and Astronomy

Approved by:

Dr. Gabor Csathy

For my parents

ACKNOWLEDGMENTS

It is with great joy that I express my gratitude to everyone who has contributed to the completion of this thesis. My acknowledgements are not limited to the people on this page, however this dissertation would not have seen the light of day without them.

My advisor, Martin Kruczenski, who with great generosity and kindness taught me the ins and outs of doing research. Whatever is of merit in this dissertation is due to his support, encouragement and guidance.

All my teachers at the physics department, especially Sherwin Love and Sergei Khlebnikov who taught wonderful courses, and first introduced me to several important topics in theory.

Everyone who attended the HEP AMO journal club, for the invaluable discussions. Especially Chen-Lung Hung and Qi Zhou without whom I would not have learnt so much about AMO physics, and Nima Lashkari for showing an interest in my work and asking questions that led me to think more deeply about what I was doing.

The physics department, Keck Foundation and DOE for financial support.
Friends at the university - Raja, Amandeep, Rishabh, Akhil, Abhilash, Jared, Debasmita, Arnesh, Kevin, Sayan, and Keiichiro for interesting discussions.

Deepika, a true *mittā*, without whom neither this dissertation would have begun, nor finished. Also, Smoky whose four paws and cold nose followed me everywhere.

Ven. Yuttadhammo Bhikkhu, who introduced me to Buddhist meditation teachings and practice.

To my parents for bringing me up with an appreciation of knowledge. Their and my sister's support has been unfailing.

Finally, I thank anyone reading this dissertation for taking an interest in this topic. I wish you happiness and peace.

Look upon the world as empty,

Mogharājā, ever mindful.

TABLE OF CONTENTS

LIST OF FIGURES

ABBREVIATIONS

BH	Bose Hubbard
CA	complexity = action
CV	complexity = volume
Eq	Equation
FG	Fefferman-Graham
RG	Renormalization Group
WdW	Wheeler de Witt

ABSTRACT

Complexity has played an increasingly important role in recent years. In this dissertation, we study some notions of complexity in systems that exhibit critical behaviour. Our results show that complexity as it is generally understood in holographic and lattice models of criticality can have several ambiguities. But despite these ambiguities, there are some features that are universally true. On the phase diagram of the system, it is the critical point which has the most complex ground state. States of physical systems with a large complexity tend to be hard to simulate using quantum circuits. Near the critical point, there is a part of complexity which is non-analytic and scales universally, i.e, the scaling is independent of the microscopic details of the Hamiltonian but depends only on the dimensionality of the system, and of the deforming operator. The coefficient of this term is unambiguous, i.e, it is not affected by the various changes in the definition of complexity which plague all the analytic terms near the critical point. We show this in lattice, field-theoretic and holographic calculations. These results were first presented in the studies [1], [2].

1. INTRODUCTION

In this dissertation, we study some aspects of complexity by studying it in specific situations, namely, near critical points. We start by discussing some preliminaries in this chapter. In the following chapters, we apply these ideas to get estimates for the complexity of states in various systems, as they approach critical behavior.

These preliminary aspects are useful to understand the different avatars that complexity has taken in recent research. They were inherited from the discipline of computational complexity in computer science. Operationally, we want to quantify the "hardness" of a certain task using complexity. Given the following notions :

- a physical system and a space of states [1]
- a simple reference state or operation
- simple operations on the space of states
- a task, for example to prepare a certain target state

then, by complexity is loosely meant the minimum number of simple operations that achieve the task or some other measure of it, for example see [3], [4]. A scenario to better understand this idea is a computational model of qubits. Here, the complexity is usually related to the minimum number of simple gates that a quantum circuit requires to create some target state or unitary. Consider N qubits with a space of states of dimension 2^N. A general state has the form

$$|\Psi\rangle = \sum_{i=1}^{2^N} \psi_i |i\rangle \tag{1.1}$$

where the complex numbers ψ_i satisfy $\sum_i |\psi_i|^2 = 1$, and the set of states $\{|i\rangle\}$ form an orthonormal basis. A possible task could be constructing a target unitary operation U on the space of qubits to some desired accuracy from some reference unitary. Such unitaries are usually built from more basic building blocks called universal gates which act as simple operations. A universal set of these gates can construct any unitary to arbitrary precision.

[1] ↑The space of states can be a restricted space instead of the full set of all allowed states of the system.

Many such sets are known. One famous example involves a set involving three one-qubit gates and a CNOT two-qubit gate [5]. Such a complexity derived from the minimal length of a quantum circuit that approximates a unitary to a given precision is known as unitary complexity $C(U)$.

Another useful notion would be that of state complexity $C(\Psi)$, which can be thought of as the minimisation over all unitary complexities for operators U that connect the reference and the target states $|R\rangle$ and $|\Psi\rangle$ respectively

$$C(|\Psi\rangle, |R\rangle) = \min_{|\Psi\rangle = U|R\rangle} C(U) \tag{1.2}$$

Usually, the label $|R\rangle$ is dropped and the state complexity is just labelled by the target state. We use that convention from now on. Complexity on a space like this behaves quite differently from the usual measures of distance like the inner product [6].

In the following sections in this chapter, we discuss some versions of complexity and how they have been used in different contexts. In addition, we introduce quantum phase transitions using a paradigmatic example of the Bose Hubbard (BH) model. We finish with a discussion of renormalisation group flows in models which are holographic. In subsequent chapters, we study the behaviour of complexity near critical points in these models.

1.1 Complexity in Quantum Information

If complexity is seen as minimal quantum circuit lengths, then an important notion of complexity for unitary operations was proposed by Nielsen and collaborators [7]–[9]. In their work, they propose an equivalence between the problem of finding an optimal quantum circuit for n-qubits (one with the smallest number of logical gates that performs a given operation), also called gate complexity and the problem of finding minimal length geodesics on a particular metric on the space $SU(2^n)$. Using a Riemannian metric on the space of unitaries, they show that the gate complexity is closely related to the minimal geodesic distance. This is done by suppressing directions that represent complex operations in the operation space. Complex operators are those that usually involve high weight operators. This suppression is obtained by introducing penalty factors in the metric for such operations.

Then the corresponding "Hamiltonian" that evolves the geodesic trajectory on the operation space can be carefully recreated by discrete operations, so that the subsequent errors do not compound along the trajectory. Consequently, the geodesic distance using such a metric is a good measure of the difficulty of implementing the operation on a quantum computer using relatively simple logical gates. This gives an intuitive way of defining complexity in a geometric way, and also paves the way for finding efficient quantum algorithms using geometrical methods.

1.2 Complexity in Field-theoretic and Lattice Models

By adapting the geometric approach developed by Nielsen and collaborators discussed in the previous section to quantum field theories, Myers and collaborators [10]–[12] computed the complexity of states in discretized gaussian scalar and fermion field theories relative to product states. For the ground state of a discretized gaussian scalar field theory, they obtain expressions for complexities C_κ using a family of metrics on the space of unitaries labelled by a real positive number κ,

$$C_\kappa = \frac{1}{2^\kappa} \sum_{\vec{p}} |\log(\omega_p/\omega_0)|^\kappa \tag{1.3}$$

Here $\vec{p}$ is the momentum vector, and ω_p are the normal mode frequencies. The parameter ω_0 parametrizes the reference state, which is a product state.

They derive these expressions by regulating the scalar field theory on a lattice. Once regulated, the theory resembles coupled harmonic oscillators. Then they show that circuits on this space of states can be thought of as trajectories in a group space. After assigning a metric or a cost function to this space, they find minimal length paths which act as optimal circuits. A detailed account for the scalar field can be found in the work [10].

In Chapter 2, we get a similar expression for the complexity of the Bose Hubbard ground state using a different approach. Our approach involves encoding the target and reference states in terms of qubits and then computing the qubit complexity for the system by analysing circuits on this space of qubits. We find that an approach involving the qubit complexity gives

results consistent with field-theoretic approaches, which directly compute the complexity in a field theory or lattice formalism.

We briefly note that other approaches for calculating complexity in field theories have also been discussed in the literature. Some prominent examples are the path integral complexity [13], [14] and the K-complexity [15]–[18].

Path integral complexity tries to optimize the Euclidean path-integral which formally creates a field theory state. This is done by minimising a functional of the metric on the Euclidean time variable and the spatial directions of the QFT. This minimum value of the functional corresponds to the complexity. Here, the complexity is related to the number of operations one has to do to create the state using a discretized Euclidean path integral. In the case of the ground state of a two-dimensional CFT, the functional corresponds to the Liouville action.

K-complexity is suited for looking at the intrinsic dynamics of the time evolution of a system. It is a measure of the spread of the target state in the Krylov basis. The Krylov basis is a special basis of the state space in which the Hamiltonian is tri-diagonal, and it can be found recursively given the Hamiltonian and an initial state.

1.3 Bose-Hubbard Model

In the next chapter, we study circuit complexity in the Boson Hubbard (BH) model. We introduce the BH model in this section. A model of interacting bosons with several interesting features, the BH model has two different phases : the Mott insulator (MI) and a Superfluid (SF) phase at $T = 0$. There are two different types of phase transitions between them [2]. Near the phase transitions, the correlation length is much larger than the lattice spacing. Thus, continuum field theory is a valid description of the system. At generic points on the phase diagram where the transition occurs, the system is described by the Gross-Pitaevskii model but at specific points, the system develops additional symmetries and the transition is in the universality class of the O(2) model. This happens when we move from one phase to another with the density fixed to an integer value.

[2]↑A quantum phase transition happens when the ground state depends non-analytically on a coupling g. Here, g usually controls the relative strength of a term in the Hamiltonian [19]–[21].

The lattice model is given by the Hamiltonian $\mathcal{H}_{BH}$ [22]

$$\mathcal{H}_{BH} = -J \sum_{<i,j>} b_i^\dagger b_j + \frac{U}{2} \sum_i n_i(n_i - 1) - \mu \sum_i n_i \tag{1.4}$$

where $< i, j >$ refers to a pair of neighboring sites i and j on a prescribed lattice [3]. Here, J controls the coupling between neighbors and allows hopping to occur between them, $U > 0$ controls the repulsion between the bosons at a given site and μ is the chemical potential. Note that $\mathcal{H}_{BH}$ has a global $U(1)$ (or equivalently $O(2)$) symmetry.

$$b_i \to \mathrm{e}^{i\theta} b_i \tag{1.5}$$

The hamiltonian $\mathcal{H}_{BH}$ can be derived from a bosonic hamiltonian with a background periodic potential $\mathcal{V}_0$ and a short ranged repulsive interaction $\mathcal{U}_0$ [23]

$$H = \int d^d x \psi^\dagger(x) \Big(-\frac{\hbar^2}{2m} \nabla^2 + \mathcal{V}_0(x) + \mathcal{V}_T(x) \Big) \psi(x) + \frac{\mathcal{U}_0}{2} \int d^d x \psi^\dagger(x) \psi^\dagger(x) \psi(x) \psi(x) \tag{1.6}$$

Here, the trapping potential $\mathcal{V}_T$ is slowly varying and produces spatial inhomogeneities. Keeping only the lowest energy vibrational states at the minima of the periodic potential gives the standard Bose Hubbard model with an additional inhomogeneous term ϵ_i. We set $\epsilon_i = 0$ from now on, and discuss the homogeneous version of the model. An intuitive description of the physics of this model can be obtained using a mean-field theory approach, which we apply in the next chapter.

1.4 Holographic critical points

In this section, we discuss critical systems in the context of the gauge/gravity correspondence. The gauge/gravity correspondence is a duality between two physical systems, where the two sets of degrees of freedom and the interactions between them are remarkably different. One of these involves gravity, while the other does not. Moreover, the description with gravity exists in one dimension higher. The most famous instance of this correspon-

[3] When i and j refer to different sites, both <i,j> and <j,i> are found in the sum over links.

dence is between type IIB string theory on $AdS_5 \times S_5$ with N units of five-form flux on each five-dimensional spacetime factor, and $\mathcal{N} = 4$ Super-Yang Mills theory in four spacetime dimensions with the gauge group $SU(N)$ [24]–[27].

The string theory has as its parameters :
the string coupling g_s and $\alpha^{'}/L^2$ (which is related to the string length scale l_s by $\alpha' = l_s^2$ where L is the AdS radius and also the constant radius of the S^5 factor) or equivalently $G_N^{(10)}/L^8$ [4] and $\alpha^{'}/L^2$.

Parameters in the $\mathcal{N} = 4$ Super-Yang Mills theory include :
the dimensionless gauge theory coupling g_{YM} and the t'Hooft coupling $\lambda = g_{YM}^2 N$ or equivalently λ and the group parameter N.

Then, the parameters on the two sides of the duality are related by

$$g_{YM}^2 = 4\pi g_s \tag{1.7}$$

$$\lambda = L^4/\alpha'^2 \tag{1.8}$$

$$\frac{\pi^4}{2N^2} = \frac{G_N^{(10)}}{L^8} = \frac{G_N^{(5)}}{L^3} \tag{1.9}$$

Thus, a large t'Hooft coupling suppresses the effects of a finite string length and large N suppresses quantum corrections to semi-classical gravity coming from G_N. Two commonly studied limits of this duality are the $\lambda \to \infty$, $N \to \infty$ limit known as the semi-classical gravity limit and the classical string theory limit in which $N \to \infty$ but λ is arbitrary.

The two theories which are dual are very symmetric. These symmetries match precisely, with the conformal $SO(4,2)$ symmetry of the gauge theory corresponding to the isometries of the AdS space, the global $SO(6)$ of the gauge theory corresponding to the isometries of the sphere S^5. The global supersymmetry manifests as local supersymmetry in the gravitational theory. A precise formulation of the duality is in terms of the equality of the Green's function generating functionals, atleast in the parameter regimes where these quantities can be computed. A duality like this is a concrete instance of the holographic principle [28], [29] since the conformal boundary of AdS space can be compactified so that it becomes

[4] $\uparrow G_N^{(D)}$ is Newton's gravitational constant in D dimensions.

$S^{d-1} \times R$. Then, the dual field theory surrounds the bulk spacetime and is known as the boundary theory.

Within this framework, bulk gravitational setups can be studied for theories that represent renormalisation group (RG) flows in Lorentz invariant boundary field theories. Geometries that are asymptotically AdS, with field variations over the radial coordinate are usually associated with a breaking of scale invariance in the boundary theory. The state in the dual field theory flows as one goes from the UV energy scales to IR scales. On deforming by a relevant operator as one looks at flows towards the IR, theories can flow to a new fixed point or to a gapped phase. In the bulk theory, we study asymptotically AdS backgrounds with a metric

$$ds^2 = \frac{L^2}{z^2}\left(\eta_{\mu\nu}dx^\mu dx^\nu + \frac{dz^2}{f(z)}\right) \tag{1.10}$$

in Poincare coordinates with some additional requirements on the function $f(z)$.

We require that it be of the form $f(z/\xi)$ with a correlation length scale ξ. When $z \ll \xi$, $f(z/\xi) \simeq 1$. This means that when we probe length scales smaller than ξ, the description is just that of the critical point. When z grows and becomes larger than ξ, the IR behaviour is controlled by the behaviour of $f(z/\xi)$ for $z > \xi$. In a scenario where the deformation operator $\mathcal{O}$ is modeled by turning on a bulk scalar field Φ, the mass of the field Φ is related to the conformal dimension of $\mathcal{O}$ in the bulk by the standard operator-field correspondence between gauge-invariant operators in the field theory and fields in the gravitational theory.

RG flows between fixed points, also known as domain wall geometries [30], [31] occur when we have the behaviour $f(z) \to \frac{L^2}{L_0^2} > 1$ as $z \to \infty$. In this limit, the geometry again looks like AdS in the deep interior with a new radius L_0.

When $f(z)$ diverges with a positive power of z in the $z \to \infty$ limit, we have a spacetime singularity which is typically resolved by considering extra dimensions. With the extra dimensions, the spacetime generically caps off at a finite proper distance from the boundary [32]. Such a situation is encountered when we look at RG flows to gapped theories.

In addition to the behaviour of $f(z)$ in the interior region $z > \xi$, RG flow geometries of the type in Eq. 1.10 can also be distinguished according to whether the leading deformation is source-like or vev-like near the boundary $z \to 0$.

For a scalar dual to the relevant deformation ($\Delta < d$) of the field theory, a source-like deformation has

$$\Phi = \Phi_{(s)} z^{d-\Delta} + ... \tag{1.11}$$

while a vev-like deformation has

$$\Phi = \Phi_{(v)} z^{\Delta} + ... \tag{1.12}$$

leading behaviour in the framework of standard quantization.

The scalar-gravity action

$$I[g, \Phi] = \frac{1}{16\pi G_N} \int d^{d+1}x \sqrt{-g} \left[R - \frac{1}{2} g^{AB} \partial_A \Phi \partial_B \Phi - V(\Phi) \right] \tag{1.13}$$

gives rise to the equations of motion

$$R_{AB} = \frac{1}{2} \partial_A \Phi \partial_B \Phi + \frac{1}{d-1} g_{AB} V(\Phi) \tag{1.14}$$

$$\frac{1}{\sqrt{-g}} \partial_A (\sqrt{-g} g^{AB} \partial_B \Phi) - \frac{\delta V}{\delta \Phi} = 0 \tag{1.15}$$

Near the boundary, the equation for $R_{zz} + R_{tt}$ gives,

$$z f'(z) = \frac{(d-\Delta)^2 \Phi_{(s)}^2}{d-1} z^{2(d-\Delta)} \tag{1.16}$$

Thus, the leading correction to $f(z)$ is positive.

$$f(z) = 1 + \frac{(d-\Delta)\Phi_s^2}{2(d-1)} z^{2(d-\Delta)} + ... \tag{1.17}$$

The quantity $\Phi_{(s)}$ and the correlation length in the dual field theory are related by the critical exponent ν [5]. Thus, the above equation is of the form $f(z) = 1 + (z/\xi)^{2(d-\Delta)} + ...$ [6]. Using a similar type of analysis, we get the asymptotic form

$$f(z) = 1 + \frac{\Delta}{2(d-1)} z^{2\Delta}\, \Phi_{(v)}^2 + ... \tag{1.18}$$

for vev deformations. The positivity of this leading correction in the expansion for $f(z)$ near the boundary is in fact a more general result that comes from the null energy theorem and Einstein equations. Together, they imply that $f(z)$ is monotonically increasing i.e $\partial_z f > 0$ [30], [33].

More generally, near the boundary $z << \xi$

$$f(z) = 1 + \sum_{m=2}^{\infty} c_m \big(\frac{z}{\xi}\big)^{m\alpha} + \mathcal{O}((z/\xi)^{2\Delta}) \tag{1.19}$$

with $\alpha = d - \Delta$ for source deformations and $c_2 = 1$.

Consistent solutions can be found near the boundary using power series expansions near the boundary. The coefficients in the expansion can be determined from the equations of motion, for a given potential. From the Eqns. 1.15, we get the equations

$$\frac{(d-1)f(z)}{z f'(z)} - (\Phi'(z))^2 = 0 \tag{1.20}$$

$$z^2 f(z)\left(\Phi''(z) + \frac{1}{2}\Phi'(z)\frac{f'(z)}{f(z)} - \frac{d-1}{z}\Phi'(z)\right) = L^2 \frac{\delta V(\Phi)}{\delta \Phi} \tag{1.21}$$

for functions $\Phi(z)$ and $f(z)$. We look at power series solutions when $z << \xi$ of the form

$$\Phi(z) = \tau z^{\alpha} + \sum_{k=2} \phi_k (\tau z^{\alpha})^k \tag{1.22}$$

$$f(z) = 1 + \sum_{k=1} f_k (\tau z^{\alpha})^k \tag{1.23}$$

[5]↑The relation between them is $\xi \sim \Phi_{(s)}^{-\nu}$. Also, since $\int d^d x \Phi_{(s)} O_\Delta$ is a term in the action, we have $\frac{1}{\nu} = d - \Delta$.
[6]↑When $\Delta = \mathrm{d}/2$, the leading order term in $f(z)$ near the boundary is $(z/\xi)^d (\log(z/\xi))^2$. This comes from an analysis of Einstein equations near the boundary, and the fact that the asymptotic leading order behavior of the scalar has a $z^{d/2}\log(z)$ term.

with $\tau \sim \xi^{-\alpha}$ and $\alpha = d - \Delta$ for source deformations. Then as an example, consider the cubic potential

$$V(\Phi) = \frac{-d(d-1)}{L^2} + \frac{1}{2}m^2\Phi^2 + \frac{1}{6L^2}g_3\Phi^3 \tag{1.24}$$

Plugging the series expansion in Eq. 1.23 into the equations of motion Eq. 1.21, the coefficients ϕ_k and f_k for some small k values are

$$\begin{aligned} f_1 &= 0 \\ f_2 &= \frac{\alpha}{2(d-1)} \\ \phi_2 &= \frac{-\kappa}{2\alpha(d-3\alpha)} \\ f_3 &= \frac{-2\kappa}{3\alpha(d-3\alpha)(d-1)} \\ \phi_3 &= \frac{\alpha(2\alpha-d)}{4(d-1)(d-4\alpha)} + \frac{\kappa^2}{4\alpha^2(d-4\alpha)(d-3\alpha)} \\ &\dots \end{aligned} \tag{1.25}$$

We postulate some $f(z/\xi)$ that have the correct near-boundary and deep interior behaviours. These act as toy models for holographic complexity calculations. For functions $f(z/\xi)$ that resemble domain wall geometries, consider the class of metric functions

$$f_\beta(z/\xi) = 1 + \frac{\beta(z/\xi)^\gamma}{1 + (z/\xi)^\gamma} \tag{1.26}$$

with parameters γ, β chosen in a manner consistent with the dimension of the deforming operator and the deep interior AdS radius respectively. So, for a source like deformation from the ultraviolet fixed point, $\gamma = 2(d - \Delta)$ and $\beta = \frac{L^2}{L_{IR}^2} - 1$.

Similarly, the class of functions

$$f_\beta(z/\xi) = (1 + (z/\xi)^\gamma)^\beta \tag{1.27}$$

with $\gamma = 2(d - \Delta)$ for source deformations and $\beta > 0$ determining the divergent behaviour of the function in the $z \to \infty$ limit. Later in Section 3.4, we will see that the $\mathcal{N} = 1$ RG flow [32] has a metric function of this form with $d = 4$, $\beta = 2$ and $\gamma = 2$.

1.5 Holographic Complexity

Motivated by studies of the time evolution of black holes, especially the growth of the Einstein-Rosen bridge [34]–[39], several gravitational quantities have been conjectured to be dual to the complexity of the dual field theory state. Two such quantities that we are interested in this dissertation are the maximal slice volume V_Σ, and the Wheeler-DeWitt (WdW) action I_{WDW}. There are two independent proposals for the interpretation of these quantities as complexity known in the literature as "complexity = volume" conjecture (CV) [34]–[37], and the "complexity = action" conjecture (CA) [38], [39] respectively.

The first proposal states that the volume of the maximal codimension-one bulk hypersurface Σ which asymptotes to a given fixed time slice at the boundary gives the complexity of the state defined on that time slice at the boundary. That is,

$$C_V = \max_\Sigma \left[\frac{V_\Sigma}{G_N l} \right] \tag{1.28}$$

where l is some bulk length scale usually taken to be the AdS scale L. In some cases, one needs to set l to be the horizon radius R_H. Thus, l introduces one of several ambiguities in the definition of the C_V. We discuss such ambiguities in Sec. 3.5.

Using some general arguments, it is possible to show that one of the terms that contribute to V_Σ scales like $\tau^{\nu(d-1)}$ near a critical point. In general, this is non-analytic in the deformation parameter τ and the coefficient of this term is universal. Restricting our analysis to RG flows that flow to gapped theories in the infrared, we use a simplified model of an AdS space cutoff by a hard wall at the value of the radial coordinate $z = \xi$. Since we know that a bulk scalar dual to a relevant deformation goes to 0 at the boundary and behaves like $\phi_{(s)} z^{d-\Delta}$ near the boundary for small values of z, we can see that when $z \sim \phi_{(s)}^{-1/(d-\Delta)} \sim \xi$, then $\phi \sim 1$ and the back-reaction on the metric is significant. In the case of gapped theories,

the back-reaction usually leads to the metric capping off in higher directions, which can be modelled in $(d+1)$-dimensions by a hard wall cutoff, in this case $z = \xi$. For this simple case the metric is given by g^{AdS} for $z < \xi$. The maximal volume slice with $t = 0$ at the boundary is just the co-dimension one $t = 0$ slice extending into the bulk and its volume is given by

$$V_\Sigma(\xi) = \sigma_{d-1} L^d \int_{z_0}^{\xi} dz \frac{1}{z^d} \tag{1.29}$$

Here, z_0 is a small z cutoff required because the volumes diverge as $z \to 0$. The critical point in this case is just given by pure AdS space extending all the way to $z \to \infty$, so we see that using the volume proposal

$$\begin{aligned} \delta C_V(\xi) &= C_V(\xi \to \infty) - C_V(\xi) \\ &= \frac{\sigma_{d-1} L^{d-1}}{(d-1) G_N} \frac{1}{\xi^{d-1}}. \qquad (1.30) \\ &= \frac{\sigma_{d-1} L^{d-1}}{(d-1) G_N} \tau^{\nu(d-1)} \qquad (1.31) \end{aligned}$$

Here the coefficient of the non-analytic piece is proportional to the number of degrees of freedom in the dual theory, since $G_N \sim l_P^{d-1}$ and $(L/l_P)^{d-1}$ scales like the density of the number of degrees of freedom in the dual. [7] It is also independent of z_0.

The second proposal refers to a calculation of the bulk action on a bulk region known as the WdW patch

$$C_A = \frac{I_{WdW}}{\pi \hbar} \tag{1.32}$$

The WdW patch is the domain of dependence of the maximal volume bulk slice Σ that we discussed in the CV proposal. This proposal does not have the length scale ambiguity that we saw in the CV case. As the WdW patch in general has boundaries (including null boundaries) and joints, the full action is fairly complicated. We discuss the full action in Chapter 3. We find that this prescription also gives a non-analytic part which scales just like the CV case.

[7] ↑For example, in the case of AdS_5/CFT_4, $L^3/G_N^{(5)}$ is proportional to N^2 and in AdS_3/CFT_2, $L/G_N^{(3)}$ is proportional to the central charge of the CFT.

Both the volume and the action satisfy a number of nice properties related to their time-dependence in spacetimes with AdS black holes. Once we have these definitions, it is possible to study these quantities near holographic critical points. We introduce the full action, and study the CV and CA conjectures in more detail in Chapter 3. We find a general agreement in the non-analytic scaling behaviour for both volume and the WdW action in near-critical models with the behaviour that is suggested in some lattice type calculations in Chapter 2. Moreover, we also find that only the part that exhibits non-analytic scaling in general is universal, while the analytic parts are subject to various ambiguities.

2. BOSE HUBBARD COMPLEXITY

In this chapter, we study complexity in the Bose Hubbard model in two and three spatial dimensions [1]. This model has been realised in optical lattices, and its several properties studied experimentally [40]–[44]. We compute the circuit complexity of the ground state of the system in both the MI and the SF phases. The behaviour of complexity near the SF-MI transition is of special interest. We will think of the Hamiltonian as a mean field Hamiltonian plus additional corrections which couple neighboring sites. Keeping only quadratic fluctuations, we find that the spectrum retains several features expected from the Bose Hubbard spectrum in the two different phases, and near the phase transition. We then rewrite our system in the language of qubits. For complexity, we use the notion introduced earlier in Section 1.1 - that minimal length geodesics select optimal circuits. When the reference state is a specific product state - the ground state of the mean field hamiltonian, we show that the qubit complexity C_{QC} is associated with a Bogoliubov type transformation.

We find that the complexity is peaked when the system is at a special critical point described by a relativistic field theory. Moreover, we find the near-critical behaviour of the complexity. This behaviour is different for the two different universality classes. We provide an explanation for these two results in Sec 2.5. We show that our numerical results agree with a different field theory calculation for the complexity done in [10] denoted as C_κ. We can go beyond the quadratic approximation using general scaling arguments, which suggest that the complexity measure $c_2(t)$ (which is the density of C_2) always has a term with non-analytic behaviour as $t \to t_c$, $|c_2(t) - c_2(t_c)| \sim |t - t_c|^{\nu h}$, upto possible logarithmic terms. Here we use ν for the critical exponent relating the coupling to the correlation length $\xi \sim |t - t_c|^{-\nu}$.

[1]↑We use h for lattice spatial dimension.

2.1 Mean Field Theory

We describe an approach to derive the phase diagram of the BH Hamiltonian using a mean field approximation in this section. We get the mean field Hamiltonian $\mathcal{H}_{MF}$ by minimising the expectation value

$$E(|\Psi\rangle) = \langle\Psi|\mathcal{H}_{BH}|\Psi\rangle \tag{2.1}$$

for normalised product states $|\Psi\rangle = \otimes_I |\psi\rangle_I$. Then $E(|\Psi\rangle) = \Omega\epsilon(|\psi\rangle)$[2], with

$$\epsilon(|\psi\rangle) = -Jf \langle\psi|b^\dagger|\psi\rangle \langle\psi|b|\psi\rangle + \frac{U}{2} \langle\psi|n(n-1)|\psi\rangle - \mu \langle\psi|n|\psi\rangle \tag{2.2}$$

where f are the number of nearest-neighbors for a site on the lattice. We can minimise $\epsilon(|\psi\rangle)$ subject to the constraint $\langle\psi|\psi\rangle = 1$ using a Lagrange multiplier and minimising the functional

$$\mathcal{G}(|\psi\rangle, \lambda) = \epsilon(|\psi\rangle) - \lambda(\langle\psi|\psi\rangle - 1) \tag{2.3}$$

Then, we find that the minimum energy value $\epsilon_0(\phi)$ is related to the vacuum energy of $\mathcal{H}_{MF}$ with mean field parameter ϕ subject to the self-consistency condition $\phi = \langle 0|b|0\rangle$, with $|0\rangle$ the mean field vacuum state.

$$\mathcal{H}_{MF} = -Jf(\phi b^\dagger + \phi^* b) + \frac{U}{2} n(n-1) - \mu n \tag{2.4}$$

We label the eigenstates of the mean field hamiltonian with a label α, $\alpha = 0, 1, 2 \ldots, N-1$ [3] with the energy eigenvalues given by ϵ_α^{MF}. The ground state energy is

$$\epsilon_0(\phi) = \epsilon_0^{MF} + Jf|\phi|^2 \tag{2.5}$$

[2]↑Here, Ω is the lattice size.
[3]↑A reasonable truncation of the local space N is needed for numerical computations.

When the coupling $J = 0$, the term in the MF hamiltonian breaking the $O(2)$ symmetry vanishes, and the mean field description is in fact exact. The model always exhibits the MI phase. This is a phase with zero compressibility,

$$\frac{\partial < n >}{\partial \mu} = 0 \tag{2.6}$$

energy gap Δ in the spectrum, and a density which is quantized and integer valued. This value can be calculated by evaluating the energy eigenvalues directly. The $J = 0$ MI state is given by $|n_0(\bar{\mu})\rangle$ with

$$n_0(\bar{\mu}) = 0 \quad \forall \quad \bar{\mu} < 0 \tag{2.7}$$

$$n_0(\bar{\mu}) = 1 \quad \forall \quad 0 < \bar{\mu} < 1 \tag{2.8}$$

$$n_0(\bar{\mu}) = 2 \quad \forall \quad 1 < \bar{\mu} < 2 \tag{2.9}$$

$$\dots$$

for $\bar{\mu} = \mu/U$. As we turn on the coupling J, there is a phase transition to the superfluid phase. This phase has gapless excitations and the density varies continuously across it. The minimisation procedure gives the well-known lobes labelled by $n = 0, 1, 2 \dots$ which surround the MI phase in which $\phi = 0$ on the phase diagram when it is plotted on the plane $(J/U, \mu/U)$. The SF phase $\phi \neq 0$ sits outside the lobe, while the critical point with $O(2)$ symmetry is at the tip of the lobe. For a square lattice with $h = 2$, we have $f = 4$. In terms of variables $t = Jf/U$ and $\bar{\mu}$, the locations of the tip of MI lobe were calculated in perturbation theory in [45]. We found agreement with that using our self-consistency method. For example, the $n = 1$ lobe tip is situated at $(t_c, \bar{\mu}_c) = (3 - \sqrt{8}, \sqrt{2} - 1)$ in both cases.

2.2 Qubit Encoding

In this section, we discuss a procedure for encoding physical systems into collections of qubits. We first do this for states in the Hilbert space of the physical system, and then

subsequently for operators. The Hilbert space for bosons on a lattice with Ω sites is of the form

$$|\Psi\rangle = |n_1, n_2, \ldots n_\Omega\rangle \tag{2.10}$$

Since this space is infinite-dimensional, one would require an infinite number of qubits to have a complete one-to-one mapping of the space. We look at systems where a natural cutoff is possible for the value of n_i, so that n_i can take a maximum of N values. Then the total number of bosons cannot exceed $\Omega(N-1)$ and the Hilbert space has a dimension of N^Ω. At a given site, we perform the identification

$$\begin{aligned}
|0\rangle &= |1, 0, 0, \ldots 0\rangle \\
|1\rangle &= |0, 1, 0, \ldots 0\rangle \\
&\ldots \\
|N-1\rangle &= |0, 0, 0, \ldots 1\rangle
\end{aligned}$$

keeping N qubits at that site. Out of the much larger number of qubit states, the physical sector is given by the constraint

$$\sum_{\alpha=0}^{N-1} \sigma^+_{i,\alpha}\sigma^-_{i,\alpha} = 1 \qquad \forall\, i \in \Omega \tag{2.11}$$

This approach allows us to write local bosonic operators as qubit operators using a simple prescription.

$$\mathcal{O}_i = \sum_{\alpha,\beta} \langle\beta|\, \mathcal{O}_i\, |\alpha\rangle\, \sigma^+_{i,\beta}\sigma^-_{i,\alpha} \tag{2.12}$$

Here, $\sigma^+_{i,\beta}$ is the usual Pauli operator at site i and qubit β. A similar approach to encoding finite systems into qubits in the context of quantum simulations can also be found in [46].

2.3 Fluctuations

The standard way of studying excitations in lattice systems with translation invariance is by introducing new operators labelled by wavenumbers instead of by positions. We organise

our description differently, since we study the relative complexity of the ground state of the Bose Hubbard model wrt. the ground state of mean field hamiltonian. Consider fluctuations $\Delta\mathcal{H}$ around the mean field

$$\mathcal{H}_{BH} = \mathcal{H}_{MF} + \Delta\mathcal{H} \tag{2.13}$$

$$\Delta\mathcal{H} = -J\sum_{\langle i,j\rangle} b_i^\dagger b_j + Jf\sum_i (\phi b_i^\dagger + \phi^* b_i) \tag{2.14}$$

Using the qubit encoding that we developed in Sec. 2.2, we can rewrite $\mathcal{H}_{MF}$ and $\Delta\mathcal{H}$ as [4]

$$\mathcal{H}_{MF} = \sum_{i,\alpha} \epsilon_\alpha \sigma^+_{i,\alpha}\sigma^-_{i,\alpha} \tag{2.15}$$

$$\begin{aligned}\Delta\mathcal{H} = {} & Jf\sum_{i,\alpha,\beta}(\phi B_{\alpha\beta} + \phi^* B^*_{\beta\alpha})\sigma^+_{i,\alpha}\sigma^-_{i,\beta} \\ & - J\sum_{\substack{\langle i,j\rangle \\ \alpha,\beta \\ \alpha',\beta'}} B_{\alpha\beta}B^*_{\beta'\alpha'}\sigma^+_{i,\alpha}\sigma^-_{i,\beta}\sigma^+_{j,\alpha'}\sigma^-_{j,\beta'}\end{aligned} \tag{2.16}$$

where $B_{\alpha\beta} = \langle\alpha|b^\dagger|\beta\rangle$ and α, β label the mean field eigenstates. The contributions from the mean field ground state operators $\alpha = 0$ can be seperated out from the higher order contributions by writing

$$\mathcal{H}_{BH} = \mathcal{H}^{(0)} + \mathcal{H}^{(1)} + \mathcal{H}^{(2)} + \mathcal{H}^{(3} + \mathcal{H}^{(4)} \tag{2.17}$$

[4]↑We drop the superscript MF and just use ϵ_α to refer to $\mathcal{H}_{MF}$ eigenvalues from here on.

where

$$\mathcal{H}^{(0)} = N\epsilon_0 + NJf|\phi|^2 \tag{2.18}$$

$$\mathcal{H}^{(1)} = 0 \tag{2.19}$$

$$\begin{aligned}\mathcal{H}^{(2)} = &\sum_{i,\alpha}(\epsilon_\alpha - \epsilon_0)\sigma^+_{i,\alpha}\,\sigma^-_{i,\alpha} \\ &- J\sum_{\langle ij\rangle,\alpha,\beta} B_{\alpha 0}B^*_{\beta 0}\,\sigma^+_{i,\alpha}\,\sigma^-_{i,0}\,\sigma^+_{j,0}\,\sigma^-_{j,\beta} - J\sum_{\langle ij\rangle,\alpha,\beta} B_{0\alpha}B^*_{0\beta}\,\sigma^+_{i,0}\,\sigma^-_{i,\alpha}\,\sigma^+_{j,\beta}\,\sigma^-_{j,0} \\ &- J\sum_{\langle ij\rangle,\alpha,\beta} B_{\alpha 0}B^*_{0\beta}\,\sigma^+_{i,\alpha}\,\sigma^-_{i,0}\,\sigma^+_{j,\beta}\,\sigma^-_{j,0} - J\sum_{\langle ij\rangle,\alpha,\beta} B_{0\alpha}B^*_{\beta 0}\,\sigma^+_{i,0}\,\sigma^-_{i,\alpha}\,\sigma^+_{j,0}\,\sigma^-_{j,\beta}\end{aligned} \tag{2.20}$$

and

$$\begin{aligned}\mathcal{H}^{(3)} = &J\sum_{\substack{\langle i,j\rangle,\alpha,\beta\\ \alpha',\beta'}} B_{\alpha 0}(\phi\sigma^+_{j,\beta}\,\sigma^-_{j,\beta} - B^*_{\beta'\alpha'}\sigma^+_{j,\alpha'}\,\sigma^-_{j,\beta'})\sigma^+_{i,\alpha}\,\sigma^-_{i,0} \\ &+ J\sum_{\substack{\langle i,j\rangle,\alpha,\beta\\ \alpha',\beta'}} B_{0\beta}(\phi\sigma^+_{j,\alpha}\,\sigma^-_{j,\alpha} - B^*_{\beta'\alpha'}\sigma^+_{j,\alpha'}\,\sigma^-_{j,\beta'})\sigma^+_{i,0}\,\sigma^-_{i,\beta} \\ &+ J\sum_{\substack{\langle i,j\rangle,\alpha,\beta\\ \alpha',\beta'}} B^*_{\alpha 0}(\phi^*\sigma^+_{i,\beta}\,\sigma^-_{i,\beta} - B_{\alpha'\beta'}\sigma^+_{i,\alpha'}\,\sigma^-_{j,\beta'})\sigma^+_{j,0}\,\sigma^-_{j,\alpha} \\ &+ J\sum_{\substack{\langle i,j\rangle,\alpha,\beta\\ \alpha',\beta'}} B^*_{0\alpha}(\phi^*\sigma^+_{i,\beta}\,\sigma^-_{i,\beta} - B_{\alpha'\beta'}\sigma^+_{i,\alpha'}\,\sigma^-_{i,\beta'})\sigma^+_{j,\alpha}\,\sigma^-_{i,0}\end{aligned} \tag{2.21}$$

$$\begin{aligned}\mathcal{H}^{(4)} = &-J|\phi|^2\sum_{\langle i,j\rangle\alpha,\beta}\sigma^+_{i,\alpha}\,\sigma^-_{i,\alpha}\,\sigma^+_{j,\beta}\,\sigma^-_{j,\beta} \\ &+ J\sum_{\langle i,j\rangle\alpha,\beta,\gamma}(\phi B_{\alpha\beta} + \phi^* B^*_{\beta\alpha})\sigma^+_{i,\alpha}\,\sigma^-_{i,\beta}\,\sigma^+_{j,\gamma}\,\sigma^-_{j,\gamma} \\ &- J\sum_{\substack{\langle i,j\rangle,\alpha,\beta\\ \alpha',\beta'}} B_{\alpha,\beta}B^*_{\beta'\alpha'}\sigma^+_{i,\alpha}\,\sigma^-_{i,\beta}\,\sigma^+_{j,\alpha'}\,\sigma^-_{j,\beta'}\end{aligned} \tag{2.22}$$

with the sums now running over $\alpha, \beta \neq 0$. For the rest of this section, we keep only terms to $\mathcal{O}(\sigma^2_{\alpha\neq 0})$. Now consider the composite wave-operator

$$\gamma_{k,\alpha} = \frac{1}{\sqrt{N}}\sum_j \mathrm{e}^{-ijk}\sigma^+_{j,0}\sigma^-_{j,\alpha} \tag{2.23}$$

with commutators

$$[\gamma_{k,\alpha}, \gamma^{\dagger}_{p,\beta}] = \delta_{k,p}\,\delta_{\alpha,\beta} - \frac{1}{N}\sum_{j,\gamma} \mathrm{e}^{ij(p-k)}\sigma^{+}_{j,\gamma}\sigma^{-}_{j,\gamma}\delta_{\alpha\beta} - \frac{1}{N}\sum_{j} \mathrm{e}^{ij(p-k)}\sigma^{+}_{j,\beta}\sigma^{-}_{j,\alpha} \tag{2.24}$$

$$[\gamma_{k,\alpha}, \gamma_{p,\beta}] = 0 \tag{2.25}$$

$$[\gamma^{\dagger}_{k,\alpha}, \gamma^{\dagger}_{p,\beta}] = 0 \tag{2.26}$$

We see that for a large lattice ($\Omega >> 1$) with a small number of $\alpha \neq 0$ excitations, we can ignore the higher order terms in the commutator to get the canonical form

$$[\gamma_{k,\alpha}, \gamma^{\dagger}_{p,\beta}] \approx \delta_{k,p}\delta_{\alpha,\beta} \tag{2.27}$$

In this approximation, the γ_k behave like bosonic oscillator modes. Then, we can improve the mean field solution by including $\mathcal{H}^{(2)}$

$$\begin{aligned}
\mathcal{H}^{(2)} &= \frac{1}{2}\sum_{k,\alpha\beta}\left(M_{\alpha\beta}(k)\gamma^{\dagger}_{k,\alpha}\gamma_{k,\alpha} + M^{*}_{\alpha\beta}(k)\gamma_{-k,\alpha}\gamma^{\dagger}_{-k,\beta}\right) \\
&\quad + \frac{1}{2}\sum_{k,\alpha\beta}\left(P_{\alpha\beta}(k)\gamma^{\dagger}_{k,\alpha}\gamma^{\dagger}_{-k,\beta} + P^{*}_{\alpha\beta}\gamma_{-k,\alpha}\gamma_{k,\beta}\right) \\
&= \frac{1}{2}\sum_{k}\begin{pmatrix}\gamma^{\dagger}_{k} & \gamma_{-k}\end{pmatrix}\begin{pmatrix}M(k) & P(k)\\ P^{*}(k) & M^{*}(k)\end{pmatrix}\begin{pmatrix}\gamma_{k}\\ \gamma^{\dagger}_{-k}\end{pmatrix} \\
&= \frac{1}{2}\sum_{k}\Gamma^{\dagger}_{k}\mathcal{H}(k)\Gamma_{k}
\end{aligned} \tag{2.28}$$

where

$$M_{\alpha\beta}(k) = \left[(\epsilon_{\alpha} - \epsilon_{0})\delta_{\alpha\beta} - Jf\eta_{k}(B_{\alpha 0}B^{*}_{\beta 0} + B_{0\beta}B^{*}_{0\alpha})\right] \tag{2.29}$$

$$P_{\alpha\beta}(k) = -Jf\eta_{k}\left(B_{0\alpha}B^{*}_{\beta 0} + B_{0\beta}B^{*}_{\alpha 0}\right) \tag{2.30}$$

$$\eta_{k} = \frac{1}{f}\sum_{a}\mathrm{e}^{ika} \tag{2.31}$$

The last sum is over nearest neighbors. We use a square lattice for our calculations, for which

$$\eta_k = \frac{1}{d}\sum_{j=1}^{d} \cos k_j$$

The B-matrices can also be taken to be real by by an appropriate choice of phases for the mean field eigenstates. Therefore, we see that $\mathcal{H}(k)$ is a real matrix. Finding the ground state of this hamiltonian is a well-known problem in many-body physics.

A canonical transformation can be used to find the ground state of $\mathcal{H}^{(2)}$. A canonical transformation $\Gamma_k \rightarrow \Lambda_k = G_k\Gamma_k$ has to preserve the $2(N-1)\times 2(N-1)$ matrix C, $G_kCG_k^\dagger = C$ where

$$C = \begin{pmatrix} \mathbf{1} & 0 \\ 0 & -\mathbf{1} \end{pmatrix}$$

For our case, a canonical transformation with the form

$$G_k = \begin{pmatrix} u_k & v_k \\ v_k & u_k \end{pmatrix}$$

suffices with u_k, v_k real $N-1\times N-1$ matrices. The constraint on these matrices takes the form [5]

$$\begin{aligned} uv^t &= vu^t \\ uu^t - vv^t &= \mathbf{1} \qquad \forall\, k \end{aligned} \tag{2.32}$$

where the superscript t denotes transposition of a matrix. Additionally, matrices of the form G that preserve the metric C form a group that is isomorphic to $GL(N-1,R)$. This is

[5]↑We drop the subscript k in the analysis here.

because given a matrix u_+ in $GL(N-1,R)$, we can use it and and its inverse $(u_+)^{-1}$ to construct u and v that satisfy the constraints in Eq. 2.32.

$$u = \frac{1}{2}\left(u_+ + (u_+^{-1})^t\right)$$
$$v = \frac{1}{2}\left(u_+ - (u_+^{-1})^t\right)$$

Also, $u+v$ is a matrix in $GL(N-1,R)$ because it is invertible, satisfying $(u+v)(u-v)^t = \mathbf{1}$. This can be checked by comparing the symmetric and anti-symmetric versions of this identity with the Eq. 2.32. Now, using the singular value decomposition of u_+, we can write it as the product

$$u_+ = \mathcal{O}\, \mathrm{e}^{\theta}\, \mathcal{U}^t \tag{2.33}$$

for orthogonal matrices $\mathcal{O}$ and $\mathcal{U}$. As the singular values of u_+ have to be positive, we can write the diagonal matrix in the form e^{θ} for some diagonal matrix θ. Since u_+ is of the form Eq. 2.33, the matrices u and v are of the form

$$u = \mathcal{O} \cosh\theta\, \mathcal{U}^t \tag{2.34}$$
$$v = \mathcal{O} \sinh\theta\, \mathcal{U}^t \tag{2.35}$$

Thus, G is of the form

$$G = \begin{pmatrix} \mathcal{O} & 0 \\ 0 & \mathcal{O} \end{pmatrix} \begin{pmatrix} \cosh\theta & \sinh\theta \\ \sinh\theta & \cosh\theta \end{pmatrix} \begin{pmatrix} \mathcal{U}^t & 0 \\ 0 & \mathcal{U}^t \end{pmatrix} \tag{2.36}$$

for each value of allowed k and the Hamiltonian is of the form

$$\mathcal{H}^{(2)} = \frac{1}{2}\sum_k \Lambda_k^\dagger C_k G_k^{-1} C_k \mathcal{H}_k G_k \Lambda_k \tag{2.37}$$

Next, G has to be chosen such that it diagonalises the matrix $C\mathcal{H}$ by a similarity transform

$$G^{-1} C\mathcal{H} G = \mathcal{H}_d$$

The eigenvalues of $C\mathcal{H}$ come in pairs (for example, see [47]),

$$\mathcal{H}_d = \begin{pmatrix} \omega & 0 \\ 0 & -\omega \end{pmatrix} \tag{2.38}$$

Here ω is a diagonal matrix with $(N-1)$ positive values ω_α. The ground state for the quadratic hamiltonian is annihilated by the oscillators $\lambda_{k,\alpha}$, $\lambda_{k,\alpha}\left|\Omega\right\rangle = 0$.

$$\left(\mathcal{U}_k \cosh\theta_k \mathcal{O}_k \gamma_k - \mathcal{U}_k \sinh\theta_k \mathcal{O}_k \gamma^\dagger_{-k}\right)_\alpha \left|\Omega\right\rangle = 0 \tag{2.39}$$

Defining new operators $\tilde{\gamma}_{k,\alpha} = (\mathcal{O}^t)_{\alpha\beta}\gamma_{k,\beta}$, we have a simpler expression

$$\left(\cosh\theta_{k,\alpha}\tilde{\gamma}_{k,\alpha} - \sinh\theta_{k,\alpha}\tilde{\gamma}^\dagger_{-k,\alpha}\right)\left|\Omega\right\rangle = 0 \tag{2.40}$$

This is true for every k and α. The quadratic hamiltonian after $\mathcal{H}_k$ has been diagonalised is

$$\mathcal{H}^{(2)} = \sum_{k,\alpha} \omega_{k,\alpha}\lambda^\dagger_{k,\alpha}\lambda_{k,\alpha} \tag{2.41}$$

and the normalised ground state $\left|\Omega\right\rangle$ that satisfies Eq. 2.40 is given by

$$\left|\Omega\right\rangle = \mathrm{e}^{\sum_{k,\alpha}\theta_{k,\alpha}(\tilde{\gamma}^\dagger_{k,\alpha}\tilde{\gamma}^\dagger_{-k,\alpha} - \tilde{\gamma}_{k,\alpha}\tilde{\gamma}_{-k,\alpha})}\left|0\right\rangle \tag{2.42}$$

Here $\left|0\right\rangle$ is the state annihilated by the $\gamma_{k,\alpha}$ operators or equivalently by the $\tilde{\gamma}_{k,\alpha}$ operators. For the type of lattice discussed in Sec. 2.1, we can check whether the spectrum $\omega_{k,\alpha}$ can reproduce the spectrum expected from the Bose Hubbard model, especially its behaviour near the phase transitions. For a two dimensional spatial lattice with size 100×100, we can look at the two lowest branches of the spectrum of $\mathcal{H}^{(2)}$. We truncate the local space to $N = 6$. The expected behaviour from the Mott Insulator is seen in Figure 2.1a inside the $n = 1$ lobe. We find two gapped modes corresponding to the particle and the hole type excitations moving along the lattice with momentum k_2. These are characteristic of this phase. An example of the SF type spectrum is seen in Figure 2.1b. Here we find one gapless mode with a linear dispersion relation, corresponding to the U(1) symmetry breaking in this

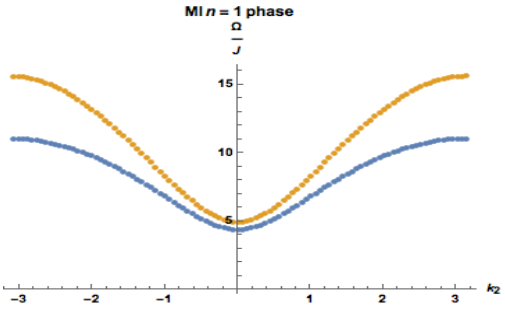

(a) $t = 0.15$, $\overline{\mu} = \sqrt{2} - 1$

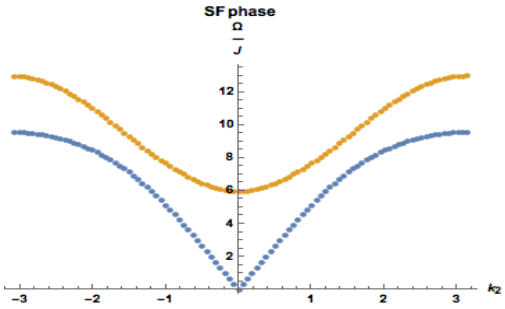

(b) $t = 0.20$, $\overline{\mu} = \sqrt{2} - 1$

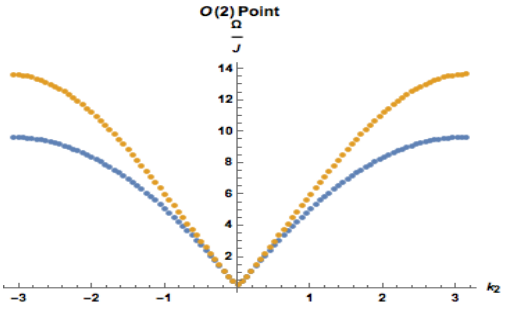

(c) $t = 3 - 2\sqrt{2}$, $\overline{\mu} = \sqrt{2} - 1$

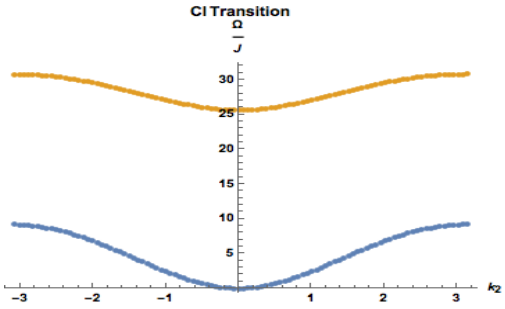

(d) $t = 0.10$, $\overline{\mu} = 0.77$

Figure 2.1. We plot ω/J for the two lowest branches of the spectrum as a function of k_2 with $k_1 = 0$ for a lattice size $\sigma_2 = 100 \times 100$ and a local Hilbert space dimension $N = 6$.

phase. Figs. 2.1c and 2.1d characterize the spectrum at the parameters corresponding to the $O(2)$ and the CI phase transition. The gapped SF mode also becomes gapless at the $O(2)$ critical point producing two linearly dispersing modes. It is known that the dynamical exponent z, $\omega_k \sim k^z$ is two at the CI phase transition [22]. We find that the lowest branch in Fig. 2.1d agrees with this for small k. We also study the kind of critical exponents the quadratic model gives us in the $O(2)$ model. The gap can be studied in two different ways near this critical point. We can fix $\bar{\mu} = \bar{\mu}_c$ and tune t to the critical value t_c, for example from within the Mott insulator phase. On the other hand, we can also look at the gap in the massive SF mode by fixing $t = t_c$ and varying $\bar{\mu}$ in the SF phase. We do this in Figure 2.2, and describe the scaling of the gap in the caption.

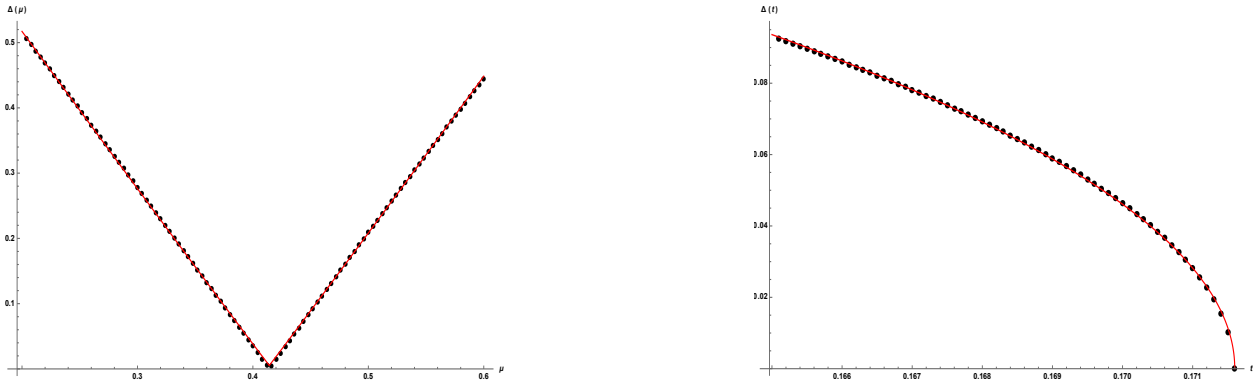

Figure 2.2. On the left, we plot the gap in the massive SF mode for $t = t_c$ and varying μ across μ_c. It fits a curve linear in $|\mu - \mu_c|$. On the right, we plot the MI gap for $\mu = \mu_c$ and varying t. It fits a curve with scaling $(t_c - t)^{1/2}$.

2.4 Circuit Complexity

The relative complexity of the target state $|\Omega\rangle$ relative to a reference state $|0\rangle$ can be thought of as the minimal circuit unitary complexity that take us from $|0\rangle$ to $|\Omega\rangle$. We want to look at unitary operators U that satisfy

$$|\Omega\rangle = U\,|0\rangle$$

and then

$$C(|\Omega\rangle) = \min_{U} C(U)$$

The path $U(\tau)$ has to be such that

$$U(0) = \mathbf{1} \tag{2.43}$$

$$U(1) = U \tag{2.44}$$

As discussed in Section 1.1, we can think of U as an unitary operation on qubits and finding the minimal geodesic distance gives us an estimate of the circuit complexity of U, $C(U)$. Formally, the path can be written as

$$U(\tau) = \hat{\mathcal{P}}\{\mathrm{e}^{-i\int_0^\tau H(\tau')d\tau'}\}$$

in terms of the "complexity hamiltonian"

$$H(\tau) = i\partial_\tau U(\tau)U^\dagger(\tau)$$

On a system of M qubits, a possible basis for $H(\tau)$ is the set of all possible strings formed from $\{(\mathbf{1}, \vec{\sigma})\}$ of size M. There are 4^M such strings, for example one such string could be $\{\sigma^+\sigma^-\mathbf{1}\sigma^3\sigma^3\mathbf{1}\sigma^-\ldots\}$.
$H(\tau)$ should then look like

$$H(\tau) = \sum_{\{\sigma\}} h_{\{\sigma\}}(\tau)V_{\{\sigma\}} \tag{2.45}$$

where the operators $V_{\{\sigma\}}$ come from the basis of strings. Then similar to Nielsen and collaborators [8], we can define a distance functional for the unitary path $U(\tau)$

$$d([U(\tau)]) = \int_0^1 dt \sqrt{\sum_{\{\sigma\}} p^2_{\{\sigma\}}|h_{\{\sigma\}}(t)|^2} \tag{2.46}$$

where we assign $p_{\{\sigma\}}$, a penalty type factor to every basis term $V_{\{\sigma\}}$. Then,

$$C_{QC}(U) = \min_{U(\tau)} d[U(\tau)] \tag{2.47}$$

We apply this approach on a lattice of qudits of dimension N. The most general one or two-qudit operator on the lattice at sites I and J can be written as

$$Q = \frac{1}{\sqrt{2}} \sum_{\substack{I,J \\ \alpha,\beta,\gamma,\delta}} \Theta_{IJ,\alpha\beta,\gamma\delta}\, \sigma^+_{I,\alpha}\, \sigma^-_{I,\beta}\, \sigma^+_{J,\gamma}\, \sigma^-_{J,\delta} + \text{h.c.} \tag{2.48}$$

This includes one-qudit operators because of the constraint in Eq. 2.11. Technically, this approach can be used to calculate the complexity for the ground state of the non-truncated hamiltonian $\mathcal{H}_{BH}$. However, we work to a quadratic approximation $\mathcal{H}^{(2)}$ for the ground state to get an estimate for the complexity. We already have one way of constructing $|\Omega\rangle$ from $|0\rangle$, using Eq. 2.42. In the previous section, we saw that this could be done using $U = \mathrm{e}^{-iH}$ with

$$H = \sum_{k,\beta\delta} i\,\theta_{k,\beta\delta}(\gamma^{\dagger}_{k,\beta}\,\gamma^{\dagger}_{-k,\delta} - \gamma_{k,\beta}\,\gamma_{-k,\delta}) \tag{2.49}$$

We see that this operator is actually formed from one and two-qudit operators of the form Eq. 2.48 with

$$\Theta_{IJ,\alpha 0\beta 0} = \sum_{k} \frac{i}{\Omega}\theta_{k,\alpha\beta}\mathrm{e}^{i(I-J)k} \tag{2.50}$$

The distance coming from this operator acts as an upper bound for the complexity. We get

$$C^2_{QC} \leq \sum_{\substack{I,J\\ \alpha,\beta}} |\Theta_{IJ,\alpha 0,\beta 0}|^2 \tag{2.51}$$

$$\leq \sum_{k,\alpha} |\theta_{k,\alpha}|^2 \tag{2.52}$$

Here, we have kept the penalty parameters very large for qudit operators with weight larger than 2, so as to suppress them in the shortest distance. We set p for other simpler operators to be 1. In fact, we think that the above upper bound acts as a good measure of the complexity since suppressing the "heavy" qudit directions using large penalties creates a Euclidean metric, in the context of which it would be hard to see how one can come up with a shorter distance for a path. Moreover, we will see that this expression is equivalent to another expression for the complexity derived in [10] by a different approach not involving qubits. Thus we have the expression for the complexity of the ground state

$$C_{QC} = \sqrt{\sum_{k,\alpha} |\theta_{k,\alpha}|^2} \tag{2.53}$$

Following the work in [10], one can define a more generic complexity

$$C_\kappa = \sum_{k,\alpha} |\theta_{k,\alpha}|^\kappa \tag{2.54}$$

Then $C_2 = C_{QC}^2$, notice that the steps in Eq. 2.52 are only valid for for C_2. We introduce the complexities $C_{\kappa\neq 2}$ here for comparison with [10]. Their interpretation in terms of Eq. 2.48 is less clear than C_2.

The expression in Eq. 1.3 for the relative state complexity can be interpreted as the complexity of the Bogoliubov transformation between two sets of oscillators. To see this, consider the oscillators

$$x_j = \sqrt{\frac{1}{2\omega_0}}(a_j + a_j^\dagger) \tag{2.55}$$

$$p_j = i\sqrt{\frac{\omega_0}{2}}(a_j^\dagger - a_j) \tag{2.56}$$

with "positions" $j = 1, 2$, and "momenta" $k = +, -$

$$x_k = \sqrt{\frac{1}{2\omega_k}}(a_k + a_k^\dagger) \tag{2.57}$$

$$p_k = i\sqrt{\frac{\omega_k}{2}}(a_k^\dagger - a_k) \tag{2.58}$$

The operators $a_{j,k}$ annihilate the state wavefunctions that act as the reference and target states $|0\rangle$ and $|\Omega\rangle$ respectively for the complexity calculation

$$a_j(x_j, \partial_j)\mathrm{e}^{-\frac{\omega_0}{2}(x_1^2+x_2^2)} = 0 \tag{2.59}$$

$$a_k(x_k, \partial_k)\mathrm{e}^{-\frac{1}{2}(\omega_+ x_+^2+\omega_- x_-^2)} = 0 \tag{2.60}$$

We can also define linear combinations

$$A_k = \sqrt{\frac{\omega_0}{2}}(x_k + \frac{i}{\omega_0}p_k) \tag{2.61}$$

with $A_\pm = \frac{a_1 \pm a_2}{2}$ and the Bogoliubov transformations

$$a_+ = \cosh\theta_+ A_+ + \sinh\theta_+ A_+^\dagger \tag{2.62}$$

$$a_- = \cosh\theta_- A_- + \sinh\theta_- q A_-^\dagger \tag{2.63}$$

Then, the complexity formula in Eq. 1.3 is just the sum of $|\theta_+|^\kappa$ and $|\theta_-|^\kappa$. This is because

$$a_+ = \sqrt{\frac{\omega_+}{2}}(x_+ + \frac{i}{\omega_+}p_+) \tag{2.64}$$

$$a_+ = \frac{1}{2}\left((\sqrt{\frac{\omega_+}{\omega_0}} + \sqrt{\frac{\omega_0}{\omega_+}})A_+ + (\sqrt{\frac{\omega_+}{\omega_0}} - \sqrt{\frac{\omega_0}{\omega_+}})A_+^\dagger\right) \tag{2.65}$$

so that $\mathrm{e}^{\theta_+} = \sqrt{\frac{\omega_+}{\omega_0}}$.

A direct application of this in a bosonic context can be found for the the well-known problem of a weakly interacting homogeneous bose gas [48] with a hamiltonian

$$H = \sum_p \frac{p^2}{2m} a_p^\dagger a_p + \frac{U_0}{2V}\sum_{p,q,r} a_{p+r}^\dagger a_{q-r}^\dagger a_p a_q \tag{2.66}$$

We can expand in $a_p, a_p^\dagger$ to quadratic order in the thermodynamic limit $N_0, N, V \to \infty$ [6] with densities fixed and non-zero, to get

$$H = E^{(0)} + \sum_{\mathbf{p}>0}[(\frac{p^2}{2m} + U)(a_p^\dagger a_p + a_{-p}^\dagger a_{-p}) + U(a_p^\dagger a_{-p}^\dagger + a_p a_{-p})] \tag{2.67}$$

with $U = nU_0$. This system is uncoupled using a Bogoliubov transformation with

$$\theta_p = \frac{1}{2}\tanh^{-1}\left(\frac{2mU}{p^2 + 2mU}\right) \tag{2.68}$$

and κ complexity

$$C_\kappa = \sum_p |\theta_p|^\kappa \approx V\int \frac{d^d p}{(2\pi)^d}|\theta(p)|^\kappa \tag{2.69}$$

[6]↑Here, we use the subscript 0 for the $p = 0$ mode. The densities are n and n_0.

For the three dimensional case, the integral gives

$$c_2^{(h=3)} = \frac{1}{48\pi}(2 - \log 4)(2mU)^{3/2} \tag{2.70}$$

The complexity for a given momentum is large when the momentum is small. In terms of the presentation of [10], this is because these modes require more scaling gates in the normal mode basis. Equivalently, we see that this is also because small momentum modes need a larger Bogoliubov transformation.

Although this calculation works for a weakly coupled gas, it does not directly carry over to the BH case. This is because the approximation in Eq. 2.67 does not capture the phase transition to the Mott Insulator phase [45].

2.5 Results

We can numerically compute the complexity for a lattice of bosons over the entire phase diagram of the BH model using the expression for the complexity. Importantly, since these fluctuations in our quadratic approximation behave like the fluctuations in the full Bose Hubbard near phase transitions, we can use our expression for the complexity to study its behaviour near the phase transition. For a large lattice, we find that the complexities C_κ increase linearly with the number of sites. We plot the complexity per site c_κ vs t for fixed $\bar{\mu}$ in Fig. 2.3 for $h = 2$.

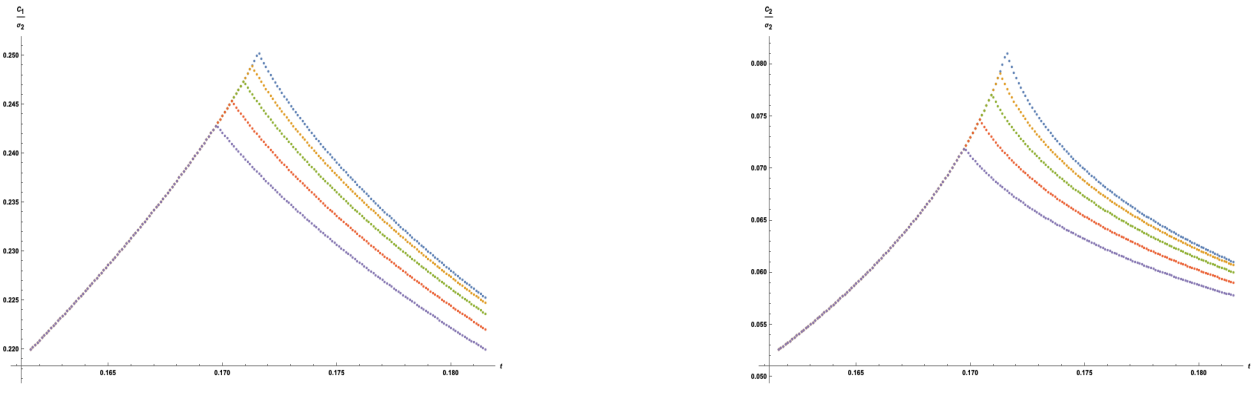

Figure 2.3. c_1 (left) and c_2 (right) vs t for fixed $\overline{\mu}$. From top to bottom, these fixed values are $\overline{\mu} = \sqrt{2} - 1, \sqrt{2} - 1.02, \sqrt{2} - 1.03, \sqrt{2} - 1.04, \sqrt{2} - 1.05$. Figures for $h = 2$ and lattice size $\sigma_2 = 100 \times 100$.

Approaching the multi-critical point at the tip of the lobe by fixing the hopping t and tuning μ is also possible. This approach is tangent to the boundary of the lobe at the critical point. The behaviour of the complexity in this case is shown in Fig. 2.4. These figures show

(a) $\kappa = 1$ complexity at fixed $t = t_c$.

(b) $\kappa = 2$ complexity at fixed $t = t_c$.

Figure 2.4. 100×100 lattice with $h = 2$.

that the ground state at the $O(2)$ critical point is the most complex in the phase diagram. This is true for both $\kappa = 1$ and $\kappa = 2$. It is also true for $h = 3$, see 2.5.

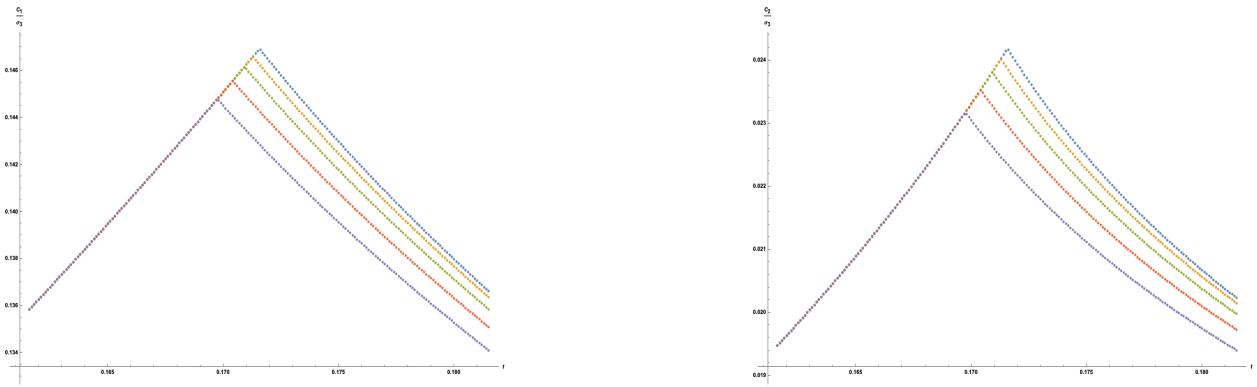

Figure 2.5. c_1 (left) and c_2 (right) for fixed $\overline{\mu}$ and varying t. The fixed $\overline{\mu}$ values are (from top to bottom) $\overline{\mu} = \sqrt{2}-1, \sqrt{2}-1.02, \sqrt{2}-1.03, \sqrt{2}-1.04, \sqrt{2}-1.05$. Here, $\sigma_3 = 20 \times 20 \times 20$ and $h = 3$.

The complexity behaves differently near the two different phase transitions in our system, and grows to larger values for the $O(2)$ phase transition. The two different universality classes have different low energy modes. We find that the complexity is also sensitive to this. The low energy modes are important because the low energy modes produce the sharp increase in the complexity near the phase transition, while the other modes act as a background since their complexity contributions are not affected by the phase transition.

Next, we study the field theoretic prediction for the complexity near a Gaussian fixed point. This is just the massless free scalar theory. The ground state complexity of this theory was already calculated by Jefferson and Myers in [10]. Their main result was that the ground state complexity defined by minimising over all unitaries that produce the target state from a fixed reference product state is given by

$$C_\kappa = \frac{1}{2^\kappa} \sum_{\vec{k}} |\log(\omega_k/\omega_0)|^\kappa \tag{2.71}$$

Here κ is a label that picks out a cost function out of several allowed cost functions. For a large lattice near the critical point $m = 0$, we study the behaviour of C_κ analytically. For our case of interest $m \sim |t - t_c|^\nu \sim 1/\xi$ and, we consider a scalar theory with two scalars. Then the complexity per spatial volume V_h is given by

$$c_\kappa = \frac{C_\kappa}{V_h} = \frac{1}{2^{\kappa-1}} \int^\Lambda \frac{d^h k}{(2\pi)^h} \left| \log\left(\frac{\sqrt{k^2+m^2}}{\omega_0}\right)\right|^\kappa \tag{2.72}$$

where Λ is the UV cutoff for the momentum integral, and Ω_{h-1} is the volume of the $(h-1)$-dimensional unit sphere S^{h-1}

$$\Omega_{h-1} = \frac{2\pi^{h/2}}{\Gamma(h/2)}$$

We can choose the reference state to be such that ω_0 is a UV parameter comparable to the cutoff Λ. A natural value for the cutoff would be when the natural log vanishes in the integrand, $\Lambda = \sqrt{\omega_0^2 - m^2}$. Then

$$c_\kappa = \frac{1}{2^{\kappa+h-2}\pi^{h/2}\Gamma(h/2)} \int_0^{\sqrt{\omega_0^2-m^2}} k^{h-1} dk \left\{ \log\left(\frac{\omega_0}{\sqrt{k^2+m^2}}\right)\right\}^\kappa \tag{2.73}$$

A direct computation for c_1 yields the expression

$$c_1 = \frac{\Omega_{h-1}}{(2\pi)^h m^2} \frac{(\omega_0^2 - m^2)^{1+h/2}}{h(h+2)} {}_2F_1[1, 1+h/2, 2+h/2, 1-\frac{\omega_0^2}{m^2}] \tag{2.74}$$

Once we know c_1, we can use that to find the higher κ complexity values. This is because of the recursion formula

$$\frac{dc_\kappa}{d\omega_0} = \frac{\kappa}{2\omega_0} c_{\kappa-1} \tag{2.75}$$

which can be written as an integral expression.

$$c_\kappa(\omega_0) = \int_m^{\omega_0} \frac{\kappa}{2\omega_0'} c_{\kappa-1}(\omega_0') d\omega_0' \tag{2.76}$$

Therefore by knowing C_{QC}, it is possible to completely reconstruct all c_κ using the recursion relations in Eqs. 2.75 and 2.76. We present the general results for c_1 and c_2.

For h even:

$$\begin{aligned} c_1 =& \frac{1}{2h}\frac{\Omega_{h-1}}{(2\pi)^h}\left\{(-1)^{\frac{h}{2}} m^h \left(-\log\frac{m^2}{\omega_0^2} + \Psi(1+\frac{h}{2}) + \gamma\right)\right. \\ &\left. + \quad \omega_0^h \sum_{n=0}^{\frac{h}{2}-1} \frac{(-1)^n}{\frac{h}{2}-n} \begin{pmatrix} h/2 \\ n \end{pmatrix} \left(\frac{m}{\omega_0}\right)^{2n}\right\} \end{aligned} \tag{2.77}$$

$$\begin{aligned} c_2 =& \frac{1}{2h}\frac{\Omega_{h-1}}{(2\pi)^h}\left\{m^h\left((-1)^{\frac{h}{2}}\ln^2\frac{\omega_0}{m} + (-1)^{\frac{h}{2}}(\Psi(1+\frac{h}{2})+\gamma)\ln\frac{\omega_0}{m}\right.\right. \\ &\left.\left. -\frac{1}{2}\sum_{n=0}^{\frac{h}{2}-1}(-1)^n \begin{pmatrix} h/2 \\ n \end{pmatrix} \frac{1}{\left(\frac{h}{2}-n\right)^2}\right) + \frac{\omega_0^h}{2}\sum_{n=0}^{\frac{h}{2}-1}(-1)^n \begin{pmatrix} h/2 \\ n \end{pmatrix} \frac{1}{\left(\frac{h}{2}-n\right)^2}\left(\frac{m}{\omega_0}\right)^{2n}\right\} \end{aligned} \tag{2.78}$$

We use Ψ for the digamma function, and γ for the Euler constant.

For h odd:

$$\begin{aligned} c_1 =& \frac{1}{4}\frac{\Omega_{h-1}}{(2\pi)^h}\left\{\omega_0^h \sum_{n=0}^{\infty}\frac{(-1)^n}{(\frac{h}{2}-n)}\frac{\Gamma(\frac{h}{2})}{n!\Gamma(\frac{h}{2}-n+1)}\left(\frac{m}{\omega_0}\right)^{2n}\right. \\ &\left. -(-1)^{\frac{h-1}{2}}\frac{2\pi}{h}m^h\right\} \end{aligned} \tag{2.79}$$

$$\begin{aligned} c_2 =& \frac{1}{4}\frac{\Omega_{h-1}}{(2\pi)^h}\left\{\frac{1}{2}\omega_0^h\sum_{n=0}^{\infty}\frac{(-1)^n}{n!}\frac{\Gamma(\frac{h}{2})}{\Gamma(\frac{h}{2}-n+1)}\frac{1}{(\frac{h}{2}-n)^2}\left(\frac{m}{\omega_0}\right)^{2n}\right. \\ &\left. -\frac{1}{2}m^h\sum_{n=0}^{\infty}\frac{(-1)^n}{n!}\frac{\Gamma(\frac{h}{2})}{\Gamma(\frac{h}{2}-n+1)}\frac{1}{(\frac{h}{2}-n)^2} - (-1)^{\frac{h-1}{2}}\frac{2\pi}{h}m^h\ln\frac{\omega_0}{m}\right\} \end{aligned} \tag{2.80}$$

Both expressions are expansions in even powers of m but with an additional term : $m^h \ln m$ for h even, and m^h for h odd.

For $h = 2$:

$$c_1^{h=2} = \frac{1}{8\pi}\left\{\boxed{m^2 \ln m^2} - m^2 \ln \omega_0^2 - m^2 + \omega_0^2\right\} \tag{2.81}$$

$$c_2^{h=2} = \frac{1}{16\pi}\left\{\boxed{-\frac{m^2}{2}\ln^2 m^2} + m^2 \ln m^2 \ln \omega_0^2 - \frac{m^2}{2}\ln^2 \omega_0^2 + m^2 \ln \frac{m^2}{\omega_0^2} - m^2 + \omega_0^2\right\} \tag{2.82}$$

For $h = 3$:

$$\begin{aligned} c_1^{h=3} =& \frac{(\omega_0^2 - m^2)^{-1/2}}{6\pi^2}\left(\frac{\omega_0^4}{3} - \frac{5}{3}m^2\omega_0^2 + \frac{4m^2}{3} + m^3\sqrt{\omega_0^2 - m^2}\sin^{-1}\sqrt{1 - \frac{m^2}{\omega_0^2}}\right) \\ =& \frac{\omega_0^3}{18\pi^2} - \frac{m^2\omega_0}{4\pi^2} + \boxed{\frac{m^3}{12\pi}} + \mathcal{O}(m^4) \end{aligned} \tag{2.83}$$

$$c_2^{h=3} = \frac{\omega_0^3}{54\pi^2} - \frac{1}{4\pi^2}\omega_0 m^2 - \boxed{\frac{m^3}{24\pi}\ln m^2} + \frac{m^3}{36\pi}\left(\frac{3}{2}\ln \omega_0^2 - \frac{3}{2}\ln 4 + 4\right) + \mathcal{O}(m^4) \tag{2.84}$$

The quantity

$$\delta c = c(t_c) - c(t)$$

is not ω_0 independent. However, there is a cut-off independent piece which is subleading in the series expression for δc that we framed in the above equations. If we set $m \sim \sqrt{t - t_c}$, which corresponds to the Gaussian model, this piece has non-analytic behavior.

We show next that the near-critical behaviour at the O(2) fixed point using numerics agrees with expected field theory behaviors in Eq. 2.82 and 2.84 with classical exponents for $h = 2$ and $h = 3$. We find that the scaling matches, and we find the coefficients of the scaling term on both sides of the critical point. This is shown in Fig. 2.6 and Fig. 2.7.

From the different expressions for complexity, for example in Eq. 2.53, we see that momentum modes with all values of α contribute to the complexity. However near the critical point, our numerical data agrees with the field theory prediction since the increase in the total complexity comes from the increase in the complexity of the low energy modes.

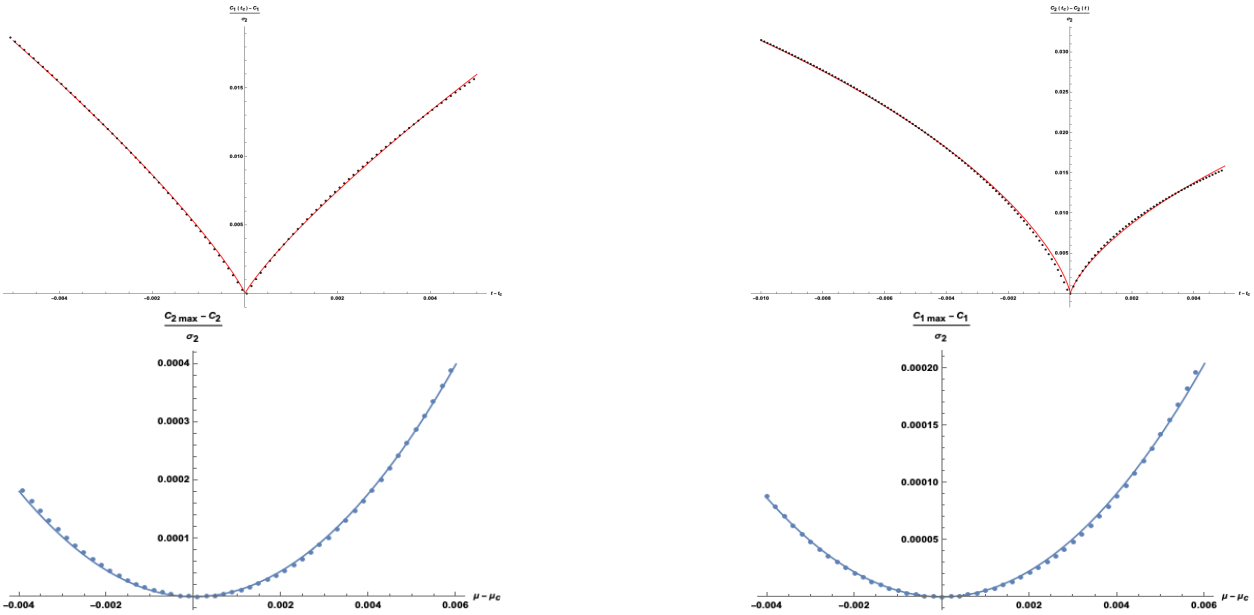

Figure 2.6. Plots for $\sigma_2 = 200 \times 200$ with the functions

(a)	$-\upsilon_{1\pm}\lvert t-t_c\rvert \log\lvert t-t_c\rvert$	$\upsilon_{1-} = 0.6968 \quad t-t_c \le 0$ $\upsilon_{1+} = 0.6039 \quad t-t_c \ge 0$
(b)	$\upsilon_{2\pm}\lvert t-t_c\rvert(\log\lvert t-t_c\rvert)^2$	$\upsilon_{2-} = 0.1467 \quad t-t_c \le 0$ $\upsilon_{2+} = 0.1129 \quad t-t_c \ge 0$
(c)	$d_{2\pm}(\mu-\mu_c)^2$	$d_{2-} = 11.3025 \quad \mu-\mu_c \le 0$ $d_{2+} = 11.0965 \quad \mu-\mu_c \ge 0$
(d)	$d_{1\pm}(\mu-\mu_c)^2$	$d_{1-} = 5.397 \quad \mu-\mu_c \le 0$ $d_{1+} = 5.67 \quad \mu-\mu_c \ge 0$

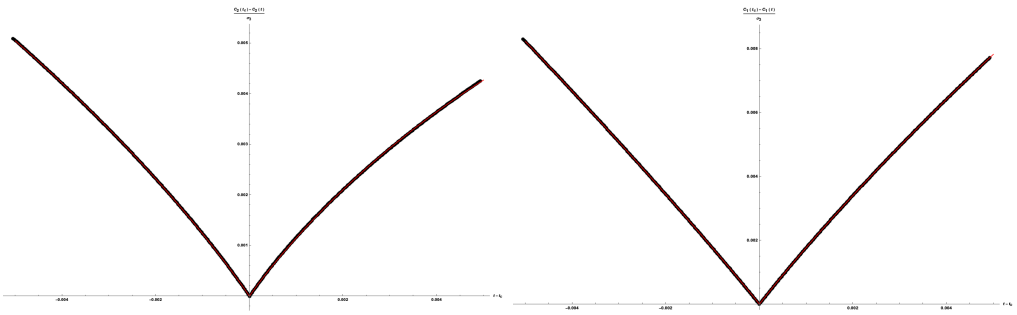

Figure 2.7. Plots for $\sigma_3 = 100 \times 100 \times 100$ with the functions

(a)	$a_\pm\lvert t-t_c\rvert + b_\pm\lvert t-t_c\rvert^{3/2}\log\lvert t-t_c\rvert$	$a_- = 1.578, \quad b_- = 1.507 \quad t-t_c \le 0$ $a_+ = 1.601, \quad b_+ = 1.978 \quad t-t_c \ge 0$
(b)	$a_\pm\lvert t-t_c\rvert + b_\pm\lvert t-t_c\rvert^{3/2}$	$a_- = 1.846, \quad b_- = -2.831 \quad t-t_c \le 0$ $a_+ = 1.944, \quad b_+ = -5.342 \quad t-t_c \ge 0$

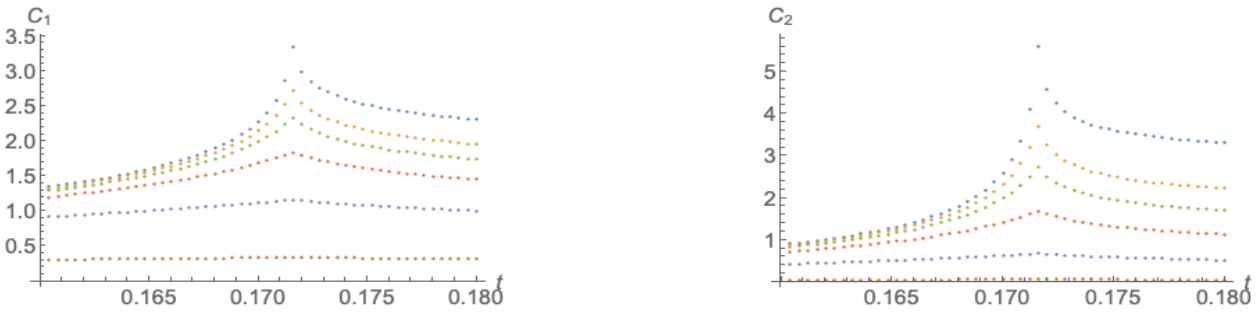

Figure 2.8. Complexity for fixed momenta and $\overline{\mu} = \overline{\mu}_c$.
The different branches have $k_1 = 0$ and, (from the bottom upwards) $k_2 = \pi/2, \pi/5, \pi/10, 3\pi/50, \pi/25, \pi/50$. The lattice has size $\sigma_2 = 100 \times 100$.

Near the critical point, the higher energy mode contributions are like a "background" for the complexity.

To see this phenomenon, we can look at the sum over flavors of the variables $|\theta_{k,\alpha}|$ with a choice of the distance functional. This gives us the complexity contributions from the different momentum k. Only the small k contributions are sensitive to $t - t_c$. This is presented in Fig. 2.8.

As we saw in Fig. 2.3 and 2.5, the complexities are independent of μ inside the Mott lobes. We check this in Fig. 2.9 by plotting the complexity inside a Mott lobe at fixed t. Whether this holds beyond the quadratic approximation is not known for the MI phase. Fig. 2.9 captures another interesting feature for the generic MI-SF transition complexity - it decreases as one enters the superfluid. The complexity contributions from the two lowest flavors is a few orders of magnitude larger than the other higher flavors. As we go from the MI to the SF phase, we plot their behaviours for a generic transition in Fig 2.10(a) and the O(2) transition in Fig. 2.10(b). From the first figure we see that even though the SF phase has a gapless mode that the MI phase does not have, the complexity still decreases as one enters the SF phase because the contribution from the massive phase decreases rapidly as its mass increases. In the second figure, we see how the two modes behave near the $O(2)$ point in contrast. As we move towards the critical point from the MI phase, the complexity from the two gapped modes increases sharply as they become massless. On the other hand,

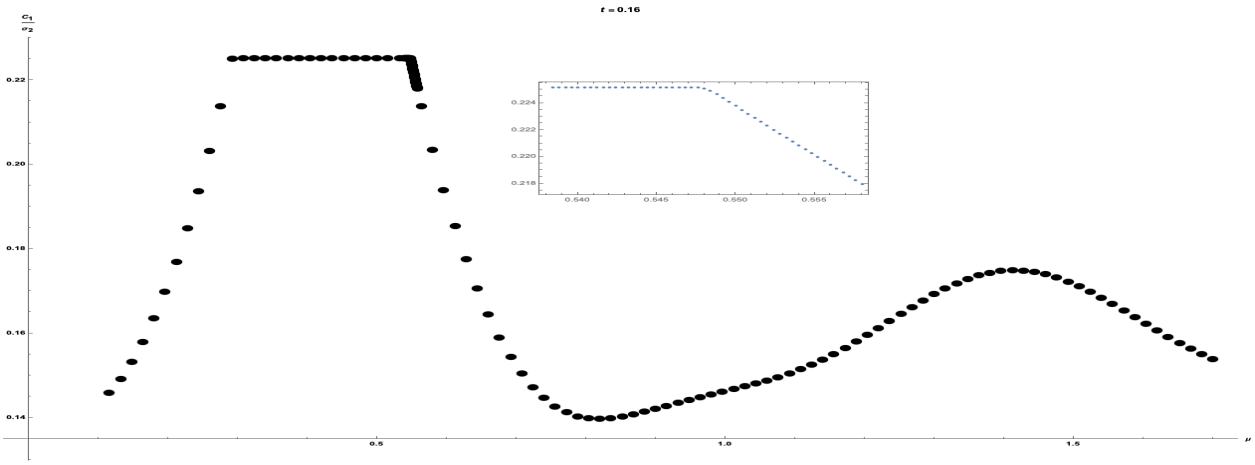

Figure 2.9. c_1 at fixed $t = 0.16$ and $\sigma_2 = 100 \times 100$. The inset shows the complexity near phase transition and a decrease in complexity here signifies the onset of superfluidity.

complexity of the massive phase decreases as its mass increases while that of the massless mode does not change significantly in the SF phase.

2.5.1 An ambiguity in the field-theoretic complexity

Based on our results for δC_κ, we find that field-theoretic complexity has some ambiguity in RG flow computations of complexity. This is because δC_κ depends on the cutoff in the Gaussian field theory case. For example we found that,

$$\delta c_1^{h=2} = \frac{1}{4\pi} \log \omega_0/m + \frac{m^2}{8\pi} \tag{2.85}$$

However, the term with universal scaling $\tau^{\nu h}$ is independent of the cutoff and unambiguous in this sense.

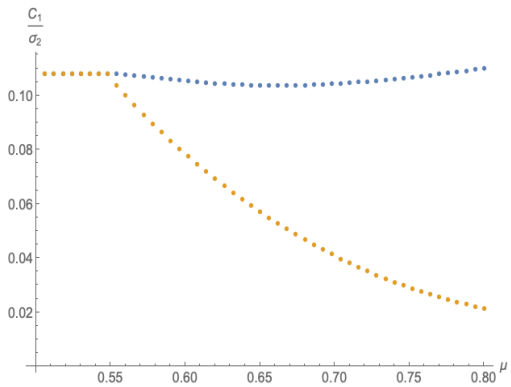

(a) c_1 for the generic transition with $t = 0.16$. The blue points capture the contribution from the mode that becomes massless in the SF while the yellow points capture the gapped mode.

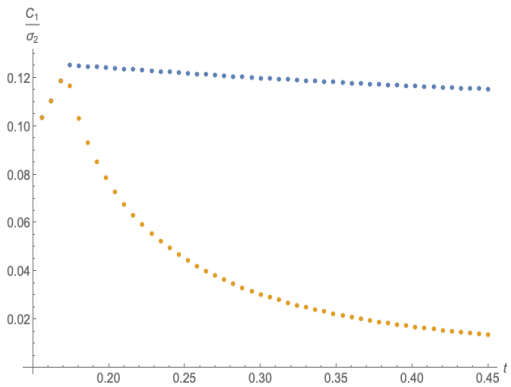

(b) c_1 at the O(2) transition with $\mu = \mu_c$. The SF has a gapped mode (yellow) and a gapless mode (blue).

Figure 2.10. $\sigma_2 = 100 \times 100$

3. HOLOGRAPHIC COMPLEXITY

In this chapter, we start by discussing the general form that calculations of volume and action take in RG flow geometries. As we have noted in the introductory chapter, these quantities are conjectured to be dual to complexity. In Section 3.1, we discuss general results related to volumes in these geometries. We show that the maximal volume V_Σ conjectured to be proprtional to complexity takes its largest value at the fixed point. We also extract the universal coefficient of the non-analytic term in the volume calculations v_0. We also compute v_0 for toy models of RG flows introduced earlier in Eq. 1.27 and 1.26. In a similar fashion, we show in Section 3.2 that the bulk part of the WdW action has a non-analytic piece with coefficient i_0, and we find that coefficient for any RG flow geometry. After that, we discuss the detailed form of the full WdW action in Section 3.3. This action has boundary and joint terms following from the geometry of the WdW spacetime. By including all these terms, we are able to compute the full WdW action I_{WdW} for the pure AdS case. We also show in this section that there are no contributions to i_0 from any boundary or joint terms, so that i_0 depends only on the bulk part of the WdW action. In Section 3.4, we compute the volume and action complexity analytically for a well-known RG flow geometry, the $\mathcal{N} = 1$ flow. We find the coefficients v_0 and i_0 for this geometry. Finally in Section 3.5, we discuss the ambiguities in holographic complexity calculations and where they come from. We conclude by discussing how they compare with the ambiguities in similar complexity calculations for black hole spacetimes.

3.1 Volume Complexity

In this section, we make some general comments about holographic complexity defined using the CV conjecture. The holographic complexity obtained from the volume conjecture is maximal at the critical point.

For the parameter $\tau \sim \xi^{-1/\nu}$, we show that

$$\frac{dV}{d\tau} < 0$$

for $\tau > 0$. The general expression for $V_\Sigma(\xi)$ is given by

$$V_\Sigma(\xi) = \frac{\sigma_{d-1} L^d}{\xi^{d-1}} \int_{z_0/\xi}^{\infty} du \frac{1}{u^d \sqrt{f(u)}} \tag{3.1}$$

for $u = z/\xi$. The cutoff is applied in a standard coordinate system - the Fefferman-Graham coordinates in which the radial coordinate has a cutoff $y = \epsilon$ [1]. This is related to the cutoff in z coordinates z_0 by

$$\ln \epsilon/\xi = \int^{z_0/\xi} du \frac{1}{u\sqrt{f(u)}} \tag{3.2}$$

where we choose the constant of integration using the fact that $z_0 = \epsilon$ when $f = 1$ and integrating by expanding $f(u)$ in a power series for small u. Differentiating

$$\begin{aligned}
&\frac{d}{d\xi}(z_0/\xi) = -\frac{z_0}{\xi^2}\sqrt{f(z_0/\xi)} \\
&\frac{dV_\Sigma}{d\xi} = \sigma_{d-1} L^d \left(-\frac{(d-1)}{\xi^d} \int_{z_0/\xi}^{\infty} du \frac{1}{u^d \sqrt{f(u)}} - \frac{\xi}{z_0^d} \frac{1}{\sqrt{f(z_0/\xi)}} \frac{d}{d\xi}(z_0/\xi) \right)
\end{aligned}$$

Combining the two equations above,

$$\frac{dV_\Sigma}{d\xi} = \frac{(d-1)\sigma_{d-1} L^d}{\xi^{d-1}} \int_{z_0/\xi}^{\infty} du \frac{1}{u^d} \left(1 - \frac{1}{\sqrt{f(u}} \right) \tag{3.3}$$

This quantity is positive because the function $f(u) \to 1$ near the boundary, and in general increases with the radial coordinate owing to its monotonicity.

Therefore

$$\frac{dV_\Sigma}{d\tau} < 0$$

Next, we show how the peak at the critical point has a non-analytic part. We start again with the general volume expression,

$$V_\Sigma[f] = \sigma_{d-1} L^d \int_{z_0}^{\infty} dz \frac{1}{z^d \sqrt{f(z/\xi)}} \tag{3.4}$$

$$= \frac{\sigma_{d-1} L^d}{\xi^{d-1}} \int_{z_0/\xi}^{\infty} du \frac{1}{u^d \sqrt{f(u)}} \tag{3.5}$$

[1] ↑See Eq. 3.55 for the general form of asymptotic AdS geometries in these coordinates.

For $z << \xi$, the radial coordinate is close to the boundary and the function $f(z)$ has an expansion

$$f(z/\xi) = 1 + \sum_{m=2}^{\infty} c_m (z/\xi)^{m\alpha} + \mathcal{O}(z/\xi)^{2\Delta} \tag{3.6}$$

for $d > \Delta > d/2$ with $\alpha = d - \Delta$ for source deformations. We can define ξ in such a way so that $c_2 = 1$. In order to extract the non-analytic term from the above integral, we introduce a constant $\delta << 1$ so that we can break the integral

$$V_\Sigma[f] = \frac{\sigma_{d-1} L^d}{\xi^{d-1}} \left[\int_{z_0/\xi}^{\delta} du \frac{1}{u^d \sqrt{f(u)}} + \int_{\delta}^{\infty} du \frac{1}{u^d \sqrt{f(u)}} \right] \tag{3.7}$$

Now we can use the series expansion in the first term while the second integral is already independent of ξ. Using $\xi = \tau^{-\nu}$, we get

$$V_\Sigma[f] = \sigma_{d-1} L^d \left[\frac{1}{(d-1) z_0^{d-1}} + \frac{1}{2} \sum_{m=2}^{\infty} \tilde{c}_m \frac{z_0^{m\alpha - d + 1}}{m\alpha - d + 1} \tau^m + \ldots + \tau^{\nu(d-1)} v_0 \right] \tag{3.8}$$

with a v_0 given by

$$v_0 = \lim_{\delta \to 0} \left(\int_{\delta}^{\infty} du \frac{1}{u^d \sqrt{f(u)}} - \frac{1}{(d-1)\delta^{d-1}} - \frac{1}{2} \sum_{m=2}^{\infty} \tilde{c}_m \frac{\delta^{m\alpha - d + 1}}{m\alpha - d + 1} + \ldots \right) \tag{3.9}$$

This limit is finite because we subtract the divergences that come from the integral. The ellipsis $(\ldots)$ in Eq. 3.8 refers to other analytic terms of the type τ^m and in Eq. 3.9 to other divergent terms in the limit $\delta \to 0$.

The result in Eq. 3.8 shows the non-analytic contribution with scaling $\tau^{\nu(d-1)}$ which is independent of the cut-off z_0. Now, if for some integer value m_0 we have $m_0 \alpha = (d-1)$ then the volume has a (non-analytic) logarithmic term $\ln \xi$. Then $\tau^{\nu(d-1)} = \tau^{m_0}$, which is analytic but still cut-off independent. We compute v_0 next for the toy models introduced in Eq. 1.26 and Eq. 1.27.

For the gapped toy model in Eq. 1.27 where β is arbitrary but positive and $d \geq 2$, we perform the integral for $V(\xi)$. It is given by

$$\frac{V_\Sigma}{\sigma_{d-1}L^d} = \frac{z_0^{1-d-\beta\gamma/2}\xi^{\beta\gamma/2}}{(d-1+\beta\gamma/2)}{}_2F_1[\frac{\beta}{2}, \frac{\beta}{2}+\frac{d-1}{\gamma}, 1+\frac{\beta}{2}+\frac{d-1}{\gamma}; -\xi^\gamma/z_0^\gamma] \tag{3.10}$$

Using the identities

$$\begin{aligned}
{}_2F_1[a,b;c;z] &= (1-z)^{-a}{}_2F_1[a,c-b;c;\frac{z}{z-1}] && (3.11)\\
{}_2F_1[a,b;c;z] &= \frac{\Gamma(c)\Gamma(c-a-b)}{\Gamma(c-a)\Gamma(c-b)}{}_2F_1[a,b;a+b+1-c;1-z] && (3.12)\\
&\quad + \frac{\Gamma(c)\Gamma(a+b-c)}{\Gamma(a)\Gamma(b)}(1-z)^{c-a-b}{}_2F_1[c-a,c-b;1+c-a-b;1-z]\\
{}_2F_1[a,b;a;z] &= (1-z)^{-b} && (3.13)
\end{aligned}$$

the maximal volume has an expansion

$$\begin{aligned}
\frac{V_\Sigma}{\sigma_{d-1}L^d} &= \frac{1}{(d-1)z_0^{d-1}} - \frac{\beta}{(d-1-\gamma)z_0^{d-1-\gamma}\xi^\gamma} + \mathcal{O}(1/z_0^{d-1-2\gamma}\xi^{2\gamma}) && (3.14)\\
&\quad + \frac{\Gamma(\frac{\beta}{2}+\frac{d-1}{\gamma})\Gamma((1-d)/\gamma)}{\gamma\Gamma(\beta/2)\xi^{d-1}}
\end{aligned}$$

Here, we get a series in powers of $\xi^{-\gamma}$ or equivalently it is a series in τ^2 which is analytic, and a universal term scaling like $\xi^{-(d-1)}$ or $\tau^{\nu(d-1)}$ which is the universal non-analytic term. This is an instance of the more general results we presented earlier. The coefficient v_0 is given by

$$v_0 = \frac{\Gamma(\frac{\beta}{2}+\frac{d-1}{\gamma})\Gamma((1-d)/\gamma)}{\gamma\Gamma(\beta/2)} \tag{3.15}$$

For toy models that have AdS domain walls in Eq. 1.26, β is related to the L_{IR} by $\beta = L^2/L_{IR}^2 - 1$ and γ to the operator dimension in the UV. The maximal volume integral can be performed analytically when $\beta \to 0$. It is given by

$$\frac{V_\Sigma}{\sigma_{d-1}L^d} = \frac{1}{(d-1)z_0^{d-1}} + \frac{\beta}{2\xi^{d-1}}\left(\frac{\pi}{\gamma}\csc\pi(1-d)/\gamma \right. \\ \left. + \frac{z_0^{\gamma+(1-d)}}{(\gamma+1-d)(\xi^\gamma+z_0^\gamma)^{1+\frac{1-d}{\gamma}}}{}_2F_1[1+\frac{1-d}{\gamma}, 1+\frac{1-d}{\gamma}, 2+\frac{1-d}{\gamma}; \frac{z_0^\gamma}{\xi^\gamma+z_0^\gamma}]\right) \tag{3.16}$$

which gives a series of analytic terms and a non-analytic term with the scaling described earlier

$$\frac{V_\Sigma}{\sigma_{d-1}L^d} = \frac{1}{(d-1)z_0^{d-1}} - \frac{\beta}{2(d-1-\gamma)}\left(\frac{1}{z_0^{d-1-\gamma}\xi^\gamma} - \frac{(\gamma+1-d)}{(2\gamma+1-d)}\frac{1}{z_0^{d-1-2\gamma}\xi^{2\gamma}} \right. \\ \left. + \mathcal{O}(\frac{1}{z_0^{d-1-3\gamma}\xi^{3\gamma}})\right) + \frac{\pi\beta}{2\gamma\xi^{d-1}}\csc\frac{\pi(1-d)}{\gamma} \tag{3.17}$$

and

$$v_0 = \frac{\pi\beta}{2\gamma}\csc\frac{\pi(1-d)}{\gamma} \tag{3.18}$$

3.2 Action Complexity

In this section, we show that the gravitational action has a non-analytic term which contributes to the complexity. The situation is analogous to the maximal volume case. This term comes from the bulk gravitational part of the WdW action [2]

$$I_{bulk} = \frac{1}{16\pi G_N}\int d^Dx\sqrt{-g}\,(R - V(0)) \tag{3.19}$$
$$= \frac{dL^{d-1}\sigma_{d-1}}{8\pi G_N}\int_{z_0}^\infty \frac{dz}{z^{d+1}\sqrt{f(z/\xi)}}\big(d-1+z\frac{df(z/\xi)}{dz} - (d+1)f(z)\big)\int_0^z \frac{dy}{\sqrt{f(y/\xi)}}$$

[2] $V(0)$ is the cosmological constant term in the action. For $D = d+1$, it is given by

$$V(0) = -\frac{d(d-1)}{L^2}$$

We use re-scaled variables $u = z/\xi$ and $w = y/\xi$

$$I_{bulk} = \frac{dL^{d-1}\sigma_{d-1}}{8\pi G_N \xi^{d-1}} \int_{z_0/\xi}^{\infty} \frac{du}{u^{d+1}\sqrt{f(u)}} \big(d - 1 + uf'(u) - (d+1)f(u)\big) \int_0^u \frac{dw}{\sqrt{f(w)}} \tag{3.20}$$

Using a constant δ between z_0/ξ and ∞ with $\delta << 1$ again, we can rewrite the bulk integral as

$$I_{bulk} = -\frac{dL^{d-1}\sigma_{d-1}}{8\pi G_N} \left(\frac{2}{(d-1)z_0^{d-1}} + \sum_{m=2}^{\infty} f_m \tau^m z_0^{m\alpha - d + 1} \right) + L^{d-1}\sigma_{d-1}\tau^{\nu(d-1)} i_0 \tag{3.21}$$

with i_0

$$i_0 = \frac{d}{8\pi G_N} \lim_{\delta \to 0} \left(\int_{\delta}^{\infty} \frac{du}{u^{d+1}\sqrt{f(u)}} \big(d - 1 + uf'(u) - (d+1)f(u)\big) \int_0^u \frac{dw}{\sqrt{f(w)}} + \frac{2}{(d-1)\delta^{d-1}} + \sum_{m=2}^{\infty} f_m \delta^{m\alpha - d + 1} \right) \tag{3.22}$$

Here f_m are some constants that can be obtained from c_m's. None of the boundary or joint gravitational terms contribute to the coefficient i_0. Thus any contribution to the non-analytic term near the fixed point comes from the bulk. We show this by directly computing the boundary terms for the general RG flow metric in the next section after introducing these various additional terms in the action.

3.3 Geometry of WdW patch

The WDW action involves computing the gravity-scalar action for RG flow solutions on the WDW patch of spacetime. This spacetime is the region formed between future and past directed light rays sent from a time slice on the boundary. Since this region has boundaries, the gravitational action also has boundary terms for it to be well-defined [49]. Such terms are generalizations of the usual Gibbons-Hawking-York terms, which are needed when the spacetime has time-like or space-like boundaries [50], [51]. In addition to co-dimension-1 boundaries, the WDW patch has codimension-2 boundaries that are joints between two codimension-1 boundaries. Joints produce special terms in the action described in [52], [53].

Since we are interested in a region between two light sheets, we also need a prescription for null boundaries [54], [55]. Here, we give a summary of all the terms that are used to compute the WdW action. The full action is given by

$$I_{WDW} = I_{bulk}(W) + I_{GHY}(\partial W_1) + I_{null}(\partial W_2) + I_{jnts}(J_1, J_2) \tag{3.23}$$

for a regularization scheme with a cutoff at $z = z_0$ as in Figure 3.1, which we sketch for AdS spacetime. ∂W_1 refers to any spacelike or timelike co-dimension one boundary, ∂W_2 to any

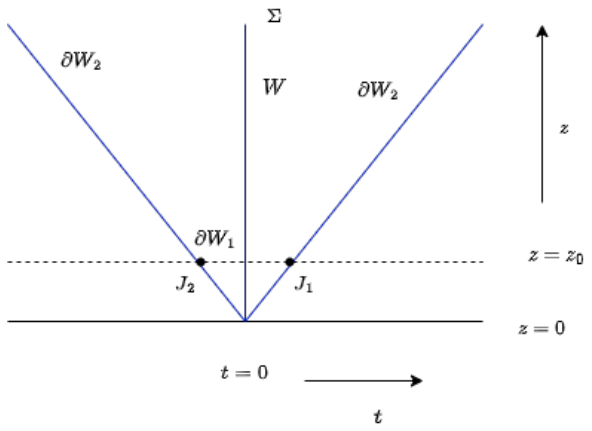

Figure 3.1. WDW region for AdS spacetime

null co-dimension one boundary and J to joints between any ∂W_1 or ∂W_2 surfaces.

The bulk part of the action involves calculating the action in Eq. 1.13 on the region W using the functions f and Φ.

The Gibbons-Hawking-York term is given by

$$I_{GHY}(\partial W_1) = \frac{1}{8\pi G_N} \int d^d x \sqrt{|h|} K \tag{3.24}$$

where h is the induced metric on ∂W_1 and K is the trace of the extrinsic curvature. [3]

The null boundaries ∂W_2 produce a contribution

$$I_{null}(\partial W_2) = -\frac{1}{8\pi G_N} \int d\lambda d^{d-1}\theta \sqrt{|\gamma|} \kappa \tag{3.25}$$

[3]↑We use the convention that normals point outwards relative to the bulk region W.

The null action depends on the parametrization of the null surface [4] through κ. This quantity is a measure of the non-affinity in the parametrization λ. In this term, γ is the metric on the $d-1$ coordinates that we label as θ. The null normal k^A satisfies

$$k^A \nabla_A k_B = \kappa k_B \tag{3.26}$$

A choice of λ (affine) can set κ to zero. We use this fact in this section to set this term to zero. In Section 3.5, we discuss non-affine choices for the parametrization, and how that affects the null term more generally.

The joint terms in the action are

$$I_{jnts}(J) = \frac{1}{8\pi G_N} \int d^{d-1}x \sqrt{\sigma} a \tag{3.27}$$

In this section, we encounter only timelike-null joints for which

$$a = -\mathsf{Sign}(k.s)\mathsf{Sign}(k.\hat{t}) \log |k.s|$$

Here k is the null normal, and s is the one-form spacelike unit normal to the timelike surface. The tangent vector $\hat{t}$ is in the tangent space of the timelike surface and, orthogonal to the junction. Also, it points outwards as in Figure 3.2a.

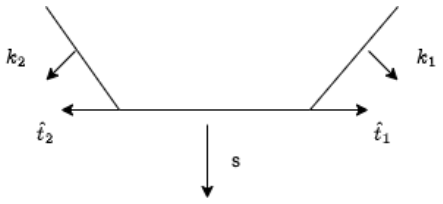

(a) Timelike-null joints

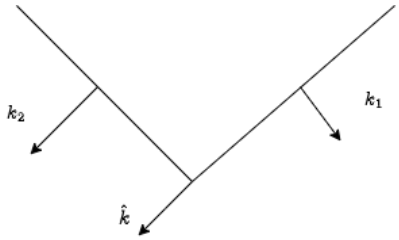

(b) Null-null joints

Figure 3.2. Joints in AdS WdW region

[4] ↑The variation of this term is not.

Using these general expressions, we calculate the WdW Action I_{WdW} for AdS_D. The scalar field $\Phi = 0$ and the metric function $f = 1$ are straightforward in this case. For AdS_D, $R = -\frac{d(d+1)}{L^2}$ giving

$$I_{bulk}(AdS_D) = -\frac{dL^{d-1}}{\kappa^2}\int_W d^D x \frac{1}{z^{d+1}} \tag{3.28}$$

The WDW region lies between the light sheets $t = \pm$. Regulating the radial direction $z = \epsilon$ for small z and $z = Z_0$ for large z, we get

$$I_{bulk}(AdS_D) = -\frac{d\sigma_{d-1}L^{d-1}}{(d-1)4\pi G_N}\left(\frac{1}{\epsilon^{d-1}} - \frac{1}{Z_0^{d-1}}\right) \tag{3.29}$$

The large z regulator can be remove. We find that I_{bulk} for AdS_D is in fact negative.

The GHY term also does not contribute at the large z regulator surface. For general $d \geq 2$, we get

$$I_{GHY}(AdS_D) = \frac{d\sigma_{d-1}L^{d-1}}{4\pi G_N}\frac{1}{\epsilon^{d-1}} \tag{3.30}$$

The null contribution can be set to zero, $I_{null} = 0$ by choosing $\kappa = 0$.

The WDW region in this case has four joints. All of these are null-timelike. The null normals in affine parametrizations are given by $dt - dz$ and $-dt - dz$ respectively. We calculate the joint action using these

$$I_{jnts}(AdS_D) = -\frac{L^{d-1}\sigma_{d-1}}{4\pi G_N}\left(\frac{\log \epsilon/L}{\epsilon^{d-1}} - \frac{\log Z_0/L}{Z_0^{d-1}}\right) \tag{3.31}$$

The large radial regulator can again be dropped. Summing up all of these terms, we get the full WdW action for AdS_{d+1}:

$$I_{WdW}(AdS_{d+1}) = \frac{\sigma_{d-1}L^{d-1}}{4\pi G_N \epsilon^{d-1}}\left(\frac{d(d-2)}{d-1} + \log L/\epsilon\right) \tag{3.32}$$

We find that this quantity is positive. This shows that the boundary terms are important for an interpretation of the action as the complexity in this context, since the complexity

has to be non-negative by definition. Computing only the bulk part would not have been adequate for this interpretation to work.

We conclude this section by showing that the boundary terms do not produce a non-analytic term in the action near a critical point. We do this by directly evaluating I_{GHY} and I_J for RG flow spacetimes. We work in the affine parametrization for the null boundaries so that $I_{null} = 0$. Both I_{GHY} and I_J come from the cutoff surface at $z = z_0$

$$I_{GHY} = \frac{d\sigma_{d-1} L^{d-1} \sqrt{f(z_0)}}{4\pi G_N z_0^d} \int_0^{z_0} \frac{dz}{\sqrt{f(z)}} \tag{3.33}$$

For small z_0, this integral is analytic in the coupling because it only gives rise to integer powers of τ.

The joint action I_J does not depend on the metric function $f(z)$. It has no ξ dependence.

$$I_J = \frac{\sigma_{d-1} L^{d-1}}{4\pi G_N z_0^{d-1}} \log L/z_0 \tag{3.34}$$

3.4 RG Flow example : $\mathcal{N} = 1$ geometry

In this section, we use a specific RG flow geometry to study holographic complexity. This is the $\mathcal{N} = 1$ geometry [32]. This RG flow geometry represents a flow from $\mathcal{N} = 4$ SYM theory in the UV to a confining theory in the IR with a mass-like source deformation. This deformation has a dimension $\Delta = 3$ in the UV. The metric function $f(z)$ and the scalar $\Phi(z)$ are given by [5]

$$f(z) = (1 + z^2/\xi^2)^2 \tag{3.35}$$

$$\Phi(z) = \frac{\sqrt{3}}{2} \log \frac{\sqrt{\xi^2 + z^2} + z}{\sqrt{\xi^2 + z^2} - z} \tag{3.36}$$

The scalar potential $V(\Phi)$ is

$$V(\Phi) = -\frac{3}{2L^2}(3 + 4\cosh(2\Phi/\sqrt{3}) + \cosh(2\Phi/\sqrt{3})^2) \tag{3.37}$$

[5]↑The correlation length ξ is different here from our previous definition by a constant factor of $\sqrt{2}$.

From the dimension Δ, we see that $\nu = 1$. The behaviour of the scalar and metric functions for $z \ll \xi$ are consistent with that.

$$f(z) = 1 + \frac{2z^2}{\xi^2} + ... \tag{3.38}$$

$$\Phi(z) = \frac{\sqrt{3}z}{\xi} + ... \tag{3.39}$$

In the limit $\xi \to \infty$, this geometry becomes AdS. Thus, we expect the maximal volumes and action to start with the AdS value when we look at expansions in z_0/ξ near the fixed point. In this model, note that $\nu(d-1) = 3$ is an integer. This means that $\tau^{\nu(d-1)} = \tau^3$ is analytic in τ. However, we will find that τ^3 term is still distinguished in series expansions for the maximal volume and action as it will be only odd term. So in that sense, it is natural to use a variable $\tilde{\tau} = \sqrt{\tau}$ in terms of which these quantities have a non-analyticity $\tilde{\tau}^{\frac{3}{2}}$ near $\tau = 0$.

3.4.1 Volume

The volume integral in Eq. 3.5 can be performed analytically and we get

$$V_\Sigma(\xi) = \sigma_3 L^4 \left(\frac{1}{3z_0^3} - \frac{1}{z_0 \xi^2} + \frac{\pi}{2\xi^3} - \frac{1}{\xi^3} \tan^{-1}(z_0/\xi) \right) \tag{3.40}$$

As we discussed below Eq. 3.38, the maximal volume expression on the right-hand side would be even under $\xi \to -\xi$ were it not for the $\frac{\pi}{2\xi^3}$ term. This term is the τ^3 term which we interpret as the universal term with coefficient v_0. For small z_0/ξ using $\xi = \tau^{-1}$ and keeping only non-vanishing terms in the $z_0 \to 0$ limit, we obtain

$$\frac{V_\Sigma(\tau)}{\sigma_3 L^4} = \frac{1}{3z_0^3} - \frac{\tau^2}{z_0} + \frac{\pi}{2}\tau^3 + \mathcal{O}(z_0) \tag{3.41}$$

We find the AdS piece, then a regulator-dependent leading term and regulator independent sub-leading term with an odd power of the coupling τ. All the terms that go to zero in the $z_0 \to 0$ contain only even powers of τ. The coefficient of the universal term is given by

$$v_0 = \frac{\pi}{2} \tag{3.42}$$

for this model.

3.4.2 Action

The scalar action has a potential term discussed before in Eq. 3.37. Evaluated on the scalar solution for the $\mathcal{N} = 1$ flow, this is given by

$$V(u) = -\frac{6}{L^2}\left(2 + 3u^2 + u^4\right) \tag{3.43}$$

for $u = z/\xi$.

We again start by regulating the geometry for both small and large values of the radial coordinate, which we call z_0 and Z_0 respectively. We define new light-cone coordinates v_1 and v_2 by the relations

$$dv_1 = dt - dz/\sqrt{f} \tag{3.44}$$

$$dv_2 = -(dt + dz/\sqrt{f}) \tag{3.45}$$

These equations can be integrated to give $v_1 = t - \xi \tan^{-1} z/\xi$ and $v_2 = -(t + \xi \tan^{-1} z/\xi)$. The region enclosed between $v_1 = 0$ and $v_2 = 0$ is the regulated WdW patch. The Eqs. 3.44, 3.45 are also useful as they give us the null normals $k_1 = k_{1\mu}dx^\mu = dv_1$ and $k_2 = k_{2\mu}dx^\mu = dv_2$ that satisfy the $\kappa = 0$ choice. They also point outwards. In terms of the familiar Poincare coordinates, the WDW region lies between the light sheets $t = \pm\xi \arctan z/\xi$ on the $t - z$ plane. Next, we calculate the action on this regulated region. The bulk term takes the form

$$I_{bulk} = \frac{\sigma_3 L^3}{8\pi G_N \xi^3}\int_{z_0/\xi}^{Z_0/\xi} du \frac{\tan^{-1} u}{u^5}\left(\frac{u^2}{2} - 8\right) \tag{3.46}$$

The large z cutoff can be taken to ∞ without any divergences and the bulk integral gives

$$I_{bulk} = \frac{\sigma_3 L^3}{8\pi G_N \xi^3}\left(-\frac{2}{3u_0^3} - \frac{1}{2u_0^4}(1 - \frac{u_0^2}{8} - \frac{9u_0^2}{2})\tan^{-1} u_0 + \frac{9}{4u_0} - \frac{9\pi}{8}\right) \tag{3.47}$$

with $u_0 = z_0/\xi$. For small u_0, we get the expansion

$$I_{bulk}(\tau) = \frac{\sigma_3 L^3}{8\pi G_N}\left(-\frac{8}{3z_0^3} + \frac{19}{6z_0}\,\tau^2 - \frac{9\pi}{8}\,\tau^3 + \mathcal{O}(z_0)\right)$$

In the $\tau \to 0$ limit, the action is given by the first term which is the AdS bulk action. Among the subleading terms, we have the universal τ^3 term which is the only odd term in τ. This has a coefficient that we called i_0.

There are two timelike boundaries for the WdW region, at the two cutoff surfaces. However, only the small z surface gives a non-vanishing GHY contribution. This contribution is

$$I_{GHY} = \frac{L^3\sigma_3}{\pi G_N}\frac{\xi \tan^{-1} z_0/\xi}{z_0^4}\left(1 + z_0^2/\xi^2\right) \tag{3.48}$$

The other surface $z = Z_0$ does not contribute as it is taken to the Poincare horizon. For small u_0

$$I_{GHY}(\tau) = \frac{L^3\sigma_3}{\pi G_N}\left(\frac{1}{z_0^3} + \frac{2}{3z_0}\,\tau^2 + \mathcal{O}(z_0)\right) \tag{3.49}$$

As we discussed earlier, this boundary piece of the action does not contribute to the coefficient i_0.

Similar to the AdS calculation, there are four null-timelike joints in this calculation. The two joints at the intersection of $z = Z_0$ surface with the null sheets do not contribute. The other two joints give

$$I_J = -\frac{\sigma_3 L^3}{4\pi G_N z_0^3}\log z_0/L \tag{3.50}$$

which also does not contribute to the i_0 coefficient. Summing up all of these contributions,

$$I_{WdW}(\tau) = \frac{\sigma_3 L^3}{8\pi G_N}\left(\frac{1}{3z_0^3}(16 + 6\log L/z_0) + \frac{17}{2z_0}\,\tau^2 - \frac{9\pi}{8}\,\tau^3 + \mathcal{O}(z_0)\right) \tag{3.51}$$

which is again positive like the AdS case with universal coefficient

$$i_0 = -\frac{9}{64 G_N} \tag{3.52}$$

3.5 Results and Ambiguities

Both the CV and the CA prescriptions give complexities that are ambiguous. In this section, we look at the various types of ambiguities that arise in the study of holographic complexity near critical points. We show that the non-analytic term that we previously calculated is free from these ambiguities, and therefore continues to be meaningful. As we have seen in specific calculations, the coefficients of the non-analytic term is not the same for the two prescriptions. The CV and the CA prescriptions [6] interpret the maximal volume and the WdW action as complexities. They allow us to therefore compute these complexities for the ground state of the $\mathcal{N} = 1$ flow. We define subtracted quantities δV_Σ and δI_{WdW}, since for small τ both the maximal volume and the action have their leading part as the AdS contribution.

$$\delta V_\Sigma = V_\Sigma(AdS_5) - V_\Sigma(\mathcal{N} = 1) \tag{3.53}$$

$$\delta I_{WdW} = I_{WdW}(AdS_5) - I_{WdW}(\mathcal{N} = 1) \tag{3.54}$$

Similar differences of volumes and actions for a finite temperature state involving a black hole have been computed before. They are known as complexities of formation. In earlier holographic calculations [49], they were found to be free of various ambiguities that arise in the calculation of the volume or the action.

[6] ↑Both the reference state and the length scale l are ambiguous. We take $l = L$ in this paper.

Since we will be comparing actions and volumes in two different asymptotically AdS geometries in this section, we apply the cutoff ϵ in the Fefferman-Graham (FG) coordinates. The metric in these coordinates is

$$ds^2 = \frac{L^2}{y^2}(dy^2 + g_{\mu\nu}(x,y)dx^\mu dx^\nu) \tag{3.55}$$

The cutoff in Poincare coordinates z_0 for a general metric function in Eq. 1.19 then has an expansion of the type

$$z_0(\epsilon) = \epsilon\left(1 + \sum_{m=2}^{\infty} \frac{d_m}{2(m\alpha+1)}\left(\frac{\epsilon}{\xi}\right)^{m\alpha} + \mathcal{O}\left((\epsilon/\xi)^{2\Delta}\right)\right) \tag{3.56}$$

with $d_2 = 1$.

This shows that z_0 is analytic in τ atleast upto the $\mathcal{O}\left((\epsilon/\xi)^{2\Delta}\right)$ term. Specifically, for the metric function corresponding to the $\mathcal{N} = 1$ flow,

$$z_0(\epsilon) = \frac{\epsilon}{\sqrt{1-\tau^2\epsilon^2}} \tag{3.57}$$

and the cutoffs in AdS and $\mathcal{N} = 1$ differ by

$$z_0(\epsilon) - \epsilon = \frac{\tau^2\epsilon^3}{2} + \mathcal{O}(\epsilon^5) \tag{3.58}$$

Using this, we write down the expressions for δC_V

$$\delta C_V = \frac{\sigma_3 L^3}{G_N}\left(\frac{3\tau^2}{2\epsilon} - \frac{\pi\tau^3}{2}\right) \tag{3.59}$$

and δC_A

$$\delta C_A = \frac{\sigma_3 L^3}{16\pi^2 G_N \hbar}\left(\frac{\tau^2}{\epsilon}(1 + 6\log L/\epsilon) + \frac{9\pi\tau^3}{4}\right) \tag{3.60}$$

In both cases, we find that $\delta C > 0$ for $\tau > 0$, which means that the critical point ground state is maximally complex. In Section 3.1, we presented this as a general result for the

volume complexity, but here we show that this result holds also for the action complexity in this specific example.

3.5.1 Choice of cutoff

Using either the CV or the CA prescriptions, we see that the complexity even after subtraction depends on the cutoff choice ϵ. This is the first ambiguity that we present in this section.

3.5.2 Joint at the cutoff surface

Instead of regulating the WdW patch using two null-timelike joints at the $z = z_0$ surface, we can regulate it using one null-null joint at the $z = z_0$ surface as shown in Figure 3.2b. This procedure also shifts the null sheets infinitesimally

$$t = \xi \tan^{-1} z/\xi - \xi \tan^{-1} z_0/\xi \tag{3.61}$$

$$t = \xi \tan^{-1} z_0/\xi - \xi \tan^{-1} z/\xi \tag{3.62}$$

for the $\mathcal{N} = 1$ case and

$$t = z - \epsilon \tag{3.63}$$

$$t = \epsilon - z \tag{3.64}$$

for the AdS case. This changes I_{bulk} and the new expressions are given by

$$I_{bulk}(AdS_5) = -\frac{\sigma_3 L^3}{12\pi G_N \epsilon^3} \tag{3.65}$$

$$I_{bulk}(\mathcal{N} = 1) = I_{bulk}(AdS_5) + \frac{\sigma_3 L^3}{8\pi G_N}\left(\frac{13}{4\epsilon}\tau^2 - \frac{9\pi}{8}\tau^3\right) \tag{3.66}$$

up to terms that vanish when $\epsilon \to 0$.

Because there is no time-like cutoff surface, the GHY action gives zero in this case. The null term is also zero by a choice $\kappa = 0$. For the null-null joint

$$a = -\mathsf{Sign}(k.\tilde{k})\mathsf{Sign}(\hat{k}.\tilde{k}) \log\left(k.\tilde{k}/2\right)$$

where $\hat{k}$ is in the tangent space of the boundary which has the normal k ($\hat{k}.k = 0$), null and pointing outwards and away from the joint while $\tilde{k}$ is the normal of the other null boundary. With this prescription, the AdS joint term is

$$I_J(AdS_5) = -\frac{\sigma_3 L^3}{4\pi G_N \epsilon^3} \log \epsilon/L \tag{3.67}$$

and the $\mathcal{N} = 1$ joint term is

$$I_J(\mathcal{N} = 1) = -\frac{\sigma_3 L^3}{4\pi G_N z_0^3} \log z_0/L \tag{3.68}$$

The two joint terms give the same joint action as that calculated from the joints in Figure 3.2a. Thus, the difference δI_J does not change. However, δI_{bulk} and δI_{GHY} are different. The quantity δC_A is still positive and given by

$$\delta C_A = \frac{3\sigma_3 L^3}{16\pi^2 G_N \hbar}\left(\frac{\tau^2}{\epsilon}(2\log L/\epsilon - 3/2) + \frac{3\pi}{4}\tau^3 + \mathcal{O}(\epsilon)\right) \tag{3.69}$$

3.5.3 Normalization and Parametrization of the null normals

Now, we discuss the ambiguity in how the null normals are normalized. For $c > 0$, so that $k_1.\hat{t} = c$ instead of 1. Then,

$$I_J(AdS_5) = -\frac{\sigma_3 L^3}{4\pi G_N \epsilon^3} \log\left(c\epsilon/L\right) \tag{3.70}$$

$$I_J(\mathcal{N} = 1) = -\frac{\sigma_3 L^3}{4\pi G_N z_0(\epsilon)^3} \log\left(c z_0(\epsilon)/L\right) \tag{3.71}$$

$$\delta I_J = \frac{\sigma_3 L^3 \tau^2}{8\pi G_N \epsilon}\left(1 + 3\log L/c\epsilon\right) \tag{3.72}$$

We find that δI retains the c dependence.

Next, we look at the null parametrization ambiguity. Consider the new parametrization $\tilde{\lambda}(\lambda)$ where λ is affine. This gives new null normals $\tilde{k_1}$ and $\tilde{k_2}$. We look at a parametrization of the type that would give rise to a constant but non-zero $\tilde{\kappa}$. Then a change in δI_{WdW} would already suggest that the action complexity has this ambiguity.

The affine parametrization λ has to satisfy

$$d\lambda = -\frac{L^2}{z^2}\frac{dz}{\sqrt{f}} \tag{3.73}$$

The null normals k_1 and k_2 corresponding to this have $\kappa = 0$. Consider $\tilde{\lambda}(\lambda)$ where λ that satisfies

$$\frac{d\tilde{\lambda}}{d\lambda} = \mathrm{e}^{-\beta} \tag{3.74}$$

The normals then satisfy $\tilde{k}^A = \mathrm{e}^{\beta}k^A$ and $\tilde{\kappa} = \frac{d}{d\tilde{\lambda}}\mathrm{e}^{\beta}$ or equivalently $\tilde{\kappa} = \frac{d}{d\tilde{\lambda}}\beta$ so that $\mathrm{e}^{\beta} = 1+\tilde{\kappa}\lambda$. The measure $\tilde{\kappa}d\tilde{\lambda} = d\beta = \frac{\tilde{\kappa}d\lambda}{1+\tilde{\kappa}\lambda}$ can be written in terms of z using Eq. 3.73. For the AdS case,

$$\mathrm{e}^{\beta} = 1 + \frac{\tilde{\kappa}L^2}{z} \tag{3.75}$$

and for the $\mathcal{N} = 1$ case,

$$\mathrm{e}^{\beta} = 1 + \frac{\tilde{\kappa}L^2}{z} + \frac{\tilde{\kappa}L^2}{\xi}\tan^{-1} z/\xi \tag{3.76}$$

The integrals for I_{null} look like

$$I_{null}(AdS_5) = \frac{\tilde{\kappa}\sigma_3 L^5}{4\pi G_N}\int_{\mathrm{e}}^{\infty}\frac{dz}{z^4(z+\tilde{\kappa}L^2)} \tag{3.77}$$

$$I_{null}(\mathcal{N}=1) = \frac{\tilde{\kappa}\sigma_3 L^5\xi^2}{4\pi G_N}\int_{z_0}^{\infty}\frac{dz}{z^5(z^2+\xi^2)(1+\tilde{\kappa}L^2/z+(\tilde{\kappa}L^2/\xi)\tan^{-1} z/\xi)} \tag{3.78}$$

The AdS integral is given by

$$I_{null}(AdS_5) = \frac{\sigma_3 L^3}{4\pi G_N}\left(\frac{1}{3\epsilon^3} - \frac{1}{2k\epsilon^2} + \frac{1}{k^2\epsilon} + \frac{1}{k^3}\log\epsilon/k\right) + \mathcal{O}(\epsilon) \tag{3.79}$$

where $\tilde{\kappa}L^2 = k$. The $\mathcal{N} = 1$ integral gives

$$I_{null}(\mathcal{N}=1) = \frac{\sigma_3 L^3}{4\pi G_N}\left(A_0 + A_2\tau^2 + A_4\tau^4 + A_5\tau^5 + \mathcal{O}(\tau^6)\right) \tag{3.80}$$

where we only keep terms upto τ^5. Keeping only terms that are non-zero in the $\epsilon \to 0$ limit, the coefficients of the various powers of τ are

$$A_0 = \frac{1}{3\epsilon^3} - \frac{1}{2k\epsilon^2} + \frac{1}{k^2\epsilon} + \frac{1}{k^3}\log\epsilon/k \tag{3.81}$$

$$A_2 = -\frac{5}{2\epsilon} - \frac{1}{2k} - \frac{3}{k}\log\epsilon/k \tag{3.82}$$

$$A_4 = \frac{k}{6}\left(-11 + 6\log tk\right) \tag{3.83}$$

$$A_5 = \frac{k^2}{12}\left(-22 + \pi + 6\pi\log 2\right) \tag{3.84}$$

For I_J, the sign does not change because e^{β} is positive definite, but the term in the logarithm changes :

$$I_J(AdS_5) = -\frac{\sigma_3 L^3}{4\pi G_N \epsilon^3}\log\left((\epsilon + k)/L\right) \tag{3.85}$$

$$I_J(\mathcal{N}=1) = -\frac{\sigma_3 L^3}{4\pi G_N z_0^3}\log\left((z_0 + k + \tau z_0 k\tan^{-1}\tau z_0)/L\right) \tag{3.86}$$

so that

$$\delta I_{null} = \frac{\sigma_3 L^3}{4\pi G_N}\left(A_2\tau^2 + A_4\tau^4 + A_5\tau^5 + \mathcal{O}(\tau^6)\right) \tag{3.87}$$

$$\delta I_J = \frac{3\sigma_3 L^3\tau^2}{16\pi G_N\epsilon}\left(1 + 2\log L/2\epsilon\right) \tag{3.88}$$

3.5.4 Functional redefinitions of the null surface

The next ambiguity is in functional redefinitions of the null surface. This comes from looking at shifts in the quantity a by constant a_0 at all the joints.

$$I_J(AdS_5) = \frac{\sigma_3 L^3}{4\pi G_N \epsilon^3}(a_0 - \log \epsilon/L) \tag{3.89}$$

$$I_J(\mathcal{N}=1) = \frac{\sigma_3 L^3}{4\pi G_N z_0^3}(a_0 - \log z_0/L) \tag{3.90}$$

$$\delta I_J = \frac{\sigma_3 L^3 \tau^2}{8\pi G_N \epsilon}(1 + 3(a_0 - \log \epsilon/L)) \tag{3.91}$$

3.5.5 Scalar boundary term

Following [56], we consider a modification by a boundary term of the scalar action.

$$I_s(\partial W_1) = \frac{1}{16\pi G_N}\int d^d x \sqrt{h}\frac{1}{2}\Phi s^A \partial_A \Phi \tag{3.92}$$

The unit normal s and the boundary region ∂W_1 were defined in Section 3.3. In a manner similar to the gravitational boundary terms, we find that this term also gives rise to analytic terms in τ for the $\mathcal{N}=1$ case. Because of this, it also does not change i_0. It is zero for AdS and $\delta I_s(\partial W_1)$ is

$$\delta I_s(\partial W_1) = \frac{3\sigma_3 L^3}{16\pi G_N}\left(\frac{\tau^2}{\epsilon} + \mathcal{O}(\epsilon)\right) \tag{3.93}$$

In summary, we see that terms in δC_A that depend on the cutoff have various other ambiguities as well. Because of this, fixing them would need several additional specifications on top of the CV and CA definitions near the critical point. On the other hand, the term that behaves like τ^3 is cutoff independent and free of all of these ambiguities. For the black hole geometry dual to the thermal state, both the volume and action calculations give a complexity of formation $\delta C(T) = C(T) - C(T=0)$ which is independent of the regularization ϵ. In fact, it can be checked that it is free of all of the ambiguities that we discussed here [49]. In this sense, these complexities of formation $\delta C(T)$ are meaningful in

the thermal case, but we here show that this does not carry over to the RG flow case of $\delta C(\tau)$. However, $\delta C(\tau)$ still does give a universal non-analytic term, which is of the same type as that found in field theoretic complexity definitions which is not affected by these ambiguities.

4. CONCLUSIONS

In this chapter, we summarize our main results and conclusions. After introducing lattice and holographic models exhibiting critical behaviour, we showed how complexity can be computed for the ground state of these models.

We find firstly that the complexity is maximal at the critical point in all cases. This is true for both holographic definitions in systems with gravity and circuit definitions in systems without gravity. From this maximum value, there is a decrease in the complexity as the system is deformed away from the critical point using coupling τ. We find that near the critical point ($\tau \neq 0$ but small), the complexity gets corrections away from the critical value. Although this correction has some ambiguities which come from how complexity is defined, we find that one can extract from it a universal term which is the coefficient in general of the only non-analytic correction term. Moreover, the scaling of this term is fixed by the dimensions of the theory and the deforming operator. We find that this scaling law holds in both theories with and without gravity, and we find this exponent for the complexity. Calculating complexity in specific cases both numerically and analytically allows us to check these general results and to calculate the universal coefficients in different cases. We find that these general results hold true in all the cases that we study - the BH model, free field theory and the holographic $\mathcal{N} = 1$ case.

REFERENCES

[1] U. Sood and M. Kruczenski, "Circuit complexity near critical points," *Journal of Physics A: Mathematical and Theoretical*, vol. 55, no. 18, p. 185 301, Apr. 2022. DOI: 10.1088/1751-8121/ac5b8f. [Online]. Available: https://doi.org/10.1088%2F1751-8121%2Fac5b8f.

[2] U. Sood and M. Kruczenski, "Non-analyticity in holographic complexity near critical points," *Journal of Physics A: Mathematical and Theoretical*, vol. 56, no. 4, p. 045 301, Jan. 2023. DOI: 10.1088/1751-8121/acb181. [Online]. Available: https://doi.org/10.1088%2F1751-8121%2Facb181.

[3] J. Watrous, *Quantum computational complexity*, 2008. arXiv: 0804.3401 [quant-ph].

[4] S. Aaronson, "The Complexity of Quantum States and Transformations: From Quantum Money to Black Holes," Jul. 2016. arXiv: 1607.05256 [quant-ph].

[5] M. A. Nielsen and I. L. Chuang, *Quantum Computation and Quantum Information: 10th Anniversary Edition*. Cambridge University Press, 2010. DOI: 10.1017/CBO9780511976667.

[6] L. Susskind, *Three lectures on complexity and black holes*, 2018. arXiv: 1810.11563 [hep-th].

[7] M. A. Nielsen, *A geometric approach to quantum circuit lower bounds*, 2005. arXiv: quant-ph/0502070 [quant-ph].

[8] M. A. Nielsen, M. R. Dowling, M. Gu, and A. C. Doherty, "Quantum computation as geometry," *Science*, vol. 311, no. 5764, pp. 1133–1135, Feb. 2006. DOI: 10.1126/science.1121541. [Online]. Available: https://doi.org/10.1126%2Fscience.1121541.

[9] M. R. Dowling and M. A. Nielsen, *The geometry of quantum computation*, 2006. arXiv: quant-ph/0701004 [quant-ph].

[10] R. A. Jefferson and R. C. Myers, "Circuit complexity in quantum field theory," *Journal of High Energy Physics*, vol. 2017, no. 10, Oct. 2017. DOI: 10.1007/jhep10(2017)107. [Online]. Available: https://doi.org/10.1007%2Fjhep10%282017%29107.

[11] L. Hackl and R. C. Myers, "Circuit complexity for free fermions," *Journal of High Energy Physics*, vol. 2018, no. 7, Jul. 2018. DOI: 10.1007/jhep07(2018)139. [Online]. Available: https://doi.org/10.1007%2Fjhep07%282018%29139.

[12] M. Guo, J. Hernandez, R. C. Myers, and S.-M. Ruan, "Circuit complexity for coherent states," *Journal of High Energy Physics*, vol. 2018, no. 10, Oct. 2018. DOI: 10.1007/jhep10(2018)011. [Online]. Available: https://doi.org/10.1007%2Fjhep10%282018%29011.

[13] T. Takayanagi, "Holographic spacetimes as quantum circuits of path-integrations," *Journal of High Energy Physics*, vol. 2018, no. 12, Dec. 2018. DOI: 10.1007/jhep12(2018)048. [Online]. Available: https://doi.org/10.1007%2Fjhep12%282018%29048.

[14] P. Caputa, N. Kundu, M. Miyaji, T. Takayanagi, and K. Watanabe, "Liouville action as path-integral complexity: From continuous tensor networks to AdS/CFT," *Journal of High Energy Physics*, vol. 2017, no. 11, Nov. 2017. DOI: 10.1007/jhep11(2017)097. [Online]. Available: https://doi.org/10.1007%2Fjhep11%282017%29097.

[15] S.-K. Jian, B. Swingle, and Z.-Y. Xian, "Complexity growth of operators in the SYK model and in JT gravity," *Journal of High Energy Physics*, vol. 2021, no. 3, Mar. 2021. DOI: 10.1007/jhep03(2021)014. [Online]. Available: https://doi.org/10.1007%2Fjhep03%282021%29014.

[16] D. E. Parker, X. Cao, A. Avdoshkin, T. Scaffidi, and E. Altman, "A universal operator growth hypothesis," *Physical Review X*, vol. 9, no. 4, Oct. 2019. DOI: 10.1103/physrevx.9.041017. [Online]. Available: https://doi.org/10.1103%2Fphysrevx.9.041017.

[17] V. Balasubramanian, P. Caputa, J. M. Magan, and Q. Wu, "Quantum chaos and the complexity of spread of states," *Physical Review D*, vol. 106, no. 4, Aug. 2022. DOI: 10.1103/physrevd.106.046007. [Online]. Available: https://doi.org/10.1103%2Fphysrevd.106.046007.

[18] J. Barbón, E. Rabinovici, R. Shir, and R. Sinha, "On the evolution of operator complexity beyond scrambling," *Journal of High Energy Physics*, vol. 2019, no. 10, Oct. 2019. DOI: 10.1007/jhep10(2019)264. [Online]. Available: https://doi.org/10.1007%2Fjhep10%282019%29264.

[19] S. Sachdev, *Quantum Phase Transitions*, 2nd ed. Cambridge University Press, 2011. DOI: 10.1017/CBO9780511973765.

[20] M. Vojta, "Quantum phase transitions," *Reports on Progress in Physics*, vol. 66, no. 12, pp. 2069–2110, Nov. 2003. DOI: 10.1088/0034-4885/66/12/r01. [Online]. Available: https://doi.org/10.1088%2F0034-4885%2F66%2F12%2Fr01.

[21] D. Voss, "How matter can melt at absolute zero," *Science*, vol. 282, no. 5387, pp. 221–224, 1998. DOI: 10.1126/science.282.5387.221. eprint: https://www.science.org/doi/pdf/10.1126/science.282.5387.221. [Online]. Available: https://www.science.org/doi/abs/10.1126/science.282.5387.221.

[22] M. P. A. Fisher, P. B. Weichman, G. Grinstein, and D. S. Fisher, "Boson localization and the superfluid-insulator transition," *Phys. Rev. B*, vol. 40, pp. 546–570, 1 Jul. 1989. DOI: 10.1103/PhysRevB.40.546. [Online]. Available: https://link.aps.org/doi/10.1103/PhysRevB.40.546.

[23] D. Jaksch, C. Bruder, J. I. Cirac, C. W. Gardiner, and P. Zoller, "Cold bosonic atoms in optical lattices," *Physical Review Letters*, vol. 81, no. 15, pp. 3108–3111, Oct. 1998. DOI: 10.1103/physrevlett.81.3108. [Online]. Available: https://doi.org/10.1103%2Fphysrevlett.81.3108.

[24] J. Maldacena, *International Journal of Theoretical Physics*, vol. 38, no. 4, pp. 1113–1133, 1999. DOI: 10.1023/a:1026654312961. [Online]. Available: https://doi.org/10.1023%2Fa%3A1026654312961.

[25] E. Witten, *Anti de sitter space and holography*, 1998. arXiv: hep-th/9802150 [hep-th].

[26] O. Aharony, S. S. Gubser, J. Maldacena, H. Ooguri, and Y. Oz, "Large n field theories, string theory and gravity," *Physics Reports*, vol. 323, no. 3-4, pp. 183–386, Jan. 2000. DOI: 10.1016/s0370-1573(99)00083-6. [Online]. Available: https://doi.org/10.1016%2Fs0370-1573%2899%2900083-6.

[27] S. Gubser, I. Klebanov, and A. Polyakov, "Gauge theory correlators from non-critical string theory," *Physics Letters B*, vol. 428, no. 1-2, pp. 105–114, May 1998. DOI: 10.1016/s0370-2693(98)00377-3. [Online]. Available: https://doi.org/10.1016%2Fs0370-2693%2898%2900377-3.

[28] L. Susskind, "The world as a hologram," *Journal of Mathematical Physics*, vol. 36, no. 11, pp. 6377–6396, Nov. 1995. DOI: 10.1063/1.531249. [Online]. Available: https://doi.org/10.1063%2F1.531249.

[29] G. t Hooft, *Dimensional reduction in quantum gravity*, 2009. arXiv: gr-qc/9310026 [gr-qc].

[30] D. Z. Freedman, S. S. Gubser, K. Pilch, and N. P. Warner, *Renormalization group flows from holography–supersymmetry and a c-theorem*, 1999. arXiv: hep-th/9904017 [hep-th].

[31] L. Girardello, M. Petrini, M. Porrati, and A. Zaffaroni, "The supergravity dual of n=1 super yangmills theory," *Nuclear Physics B*, vol. 569, no. 1-3, pp. 451–469, Mar. 2000. DOI: 10.1016/s0550-3213(99)00764-6. [Online]. Available: https://doi.org/10.1016%2Fs0550-3213%2899%2900764-6.

[32] L. Girardello, M. Petrini, M. Porrati, and A. Zaffaroni, "Novel local CFT and exact results on perturbations of in/i = 4 super yang mills from AdS dynamics," *Journal of High Energy Physics*, vol. 1998, no. 12, pp. 022–022, Dec. 1998. DOI: 10.1088/1126-6708/1998/12/022. [Online]. Available: https://doi.org/10.1088%2F1126-6708%2F1998%2F12%2F022.

[33] H. Liu and M. Mezei, "A refinement of entanglement entropy and the number of degrees of freedom," *Journal of High Energy Physics*, vol. 2013, no. 4, Apr. 2013. DOI: 10.1007/jhep04(2013)162. [Online]. Available: https://doi.org/10.1007%2Fjhep04%282013%29162.

[34] L. Susskind and Y. Zhao, "Switchbacks and the Bridge to Nowhere," Aug. 2014. arXiv: 1408.2823 [hep-th].

[35] L. Susskind, "Entanglement is not enough," *Fortsch. Phys.*, vol. 64, pp. 49–71, 2016. DOI: 10.1002/prop.201500095. arXiv: 1411.0690 [hep-th].

[36] L. Susskind, "Computational Complexity and Black Hole Horizons," *Fortsch. Phys.*, vol. 64, pp. 24–43, 2016, [Addendum: Fortsch.Phys. 64, 44–48 (2016)]. DOI: 10.1002/prop.201500092. arXiv: 1403.5695 [hep-th].

[37] D. Stanford and L. Susskind, "Complexity and Shock Wave Geometries," *Phys. Rev. D*, vol. 90, no. 12, p. 126 007, 2014. DOI: 10.1103/PhysRevD.90.126007. arXiv: 1406.2678 [hep-th].

[38] A. R. Brown, D. A. Roberts, L. Susskind, B. Swingle, and Y. Zhao, "Holographic Complexity Equals Bulk Action?" *Phys. Rev. Lett.*, vol. 116, no. 19, p. 191 301, 2016. DOI: 10.1103/PhysRevLett.116.191301. arXiv: 1509.07876 [hep-th].

[39] A. R. Brown, D. A. Roberts, L. Susskind, B. Swingle, and Y. Zhao, "Complexity, action, and black holes," *Phys. Rev. D*, vol. 93, no. 8, p. 086 006, 2016. DOI: 10.1103/PhysRevD.93.086006. arXiv: 1512.04993 [hep-th].

[40] M. Greiner, O. Mandel, T. Esslinger, T. W. Hänsch, and I. Bloch, "Quantum phase transition from a superfluid to a mott insulator in a gas of ultracold atoms," *Nature*, vol. 415, no. 6867, pp. 39–44, 2002. DOI: 10.1038/415039a. [Online]. Available: https://doi.org/10.1038/415039a.

[41] T. Stöferle, H. Moritz, C. Schori, M. Köhl, and T. Esslinger, "Transition from a strongly interacting 1d superfluid to a mott insulator," *Physical Review Letters*, vol. 92, no. 13, Mar. 2004. DOI: 10.1103/physrevlett.92.130403. [Online]. Available: https://doi.org/10.1103%2Fphysrevlett.92.130403.

[42] C. Schori, T. Stöferle, H. Moritz, M. Köhl, and T. Esslinger, "Excitations of a superfluid in a three-dimensional optical lattice," *Physical Review Letters*, vol. 93, no. 24, Dec. 2004. DOI: 10.1103/physrevlett.93.240402. [Online]. Available: https://doi.org/10.1103%2Fphysrevlett.93.240402.

[43] K. Xu, Y. Liu, J. R. Abo-Shaeer, *et al.*, "Sodium bose-einstein condensates in an optical lattice," *Phys. Rev. A*, vol. 72, p. 043 604, 4 Oct. 2005. DOI: 10.1103/PhysRevA.72.043604. [Online]. Available: https://link.aps.org/doi/10.1103/PhysRevA.72.043604.

[44] F. Gerbier, S. Fölling, A. Widera, O. Mandel, and I. Bloch, "Probing number squeezing of ultracold atoms across the superfluid-mott insulator transition," *Phys. Rev. Lett.*, vol. 96, p. 090 401, 9 Mar. 2006. DOI: 10.1103/PhysRevLett.96.090401. [Online]. Available: https://link.aps.org/doi/10.1103/PhysRevLett.96.090401.

[45] D. van Oosten, P. van der Straten, and H. T. C. Stoof, "Quantum phases in an optical lattice," *Physical Review A*, vol. 63, no. 5, Apr. 2001. DOI: 10.1103/physreva.63.053601. [Online]. Available: https://doi.org/10.1103%2Fphysreva.63.053601.

[46] R. D. Somma, G. Ortiz, E. H. Knill, and J. Gubernatis, "Quantum simulations of physics problems," Aug. 2003. DOI: 10.1117/12.487249. [Online]. Available: https://doi.org/10.1117%2F12.487249.

[47] S. Ripka, J. Blaizot, and G. Ripka, *Quantum Theory of Finite Systems*. MIT Press, 1986, ISBN: 9780262022149. [Online]. Available: https://books.google.com/books?id=s%5C_xlQgAACAAJ.

[48] L. Landau, E. Lifshits, and L. Pitaevski, *Statistical Physics*, ser. Course of theoretical physics pt. 2. Pergamon Press, 1980, ISBN: 9780080230733. [Online]. Available: https://books.google.com/books?id=KAlRAAAAMAAJ.

[49] S. Chapman, H. Marrochio, and R. C. Myers, "Complexity of formation in holography," *Journal of High Energy Physics*, vol. 2017, no. 1, Jan. 2017. DOI: 10.1007/jhep01(2017)062. [Online]. Available: https://doi.org/10.1007%2Fjhep01%282017%29062.

[50] G. W. Gibbons and S. W. Hawking, "Action integrals and partition functions in quantum gravity," *Phys. Rev. D*, vol. 15, pp. 2752–2756, 10 May 1977. DOI: 10.1103/PhysRevD.15.2752. [Online]. Available: https://link.aps.org/doi/10.1103/PhysRevD.15.2752.

[51] J. W. York Jr., "Role of conformal three geometry in the dynamics of gravitation," *Phys. Rev. Lett.*, vol. 28, pp. 1082–1085, 1972. DOI: 10.1103/PhysRevLett.28.1082.

[52] G. Hayward, "Gravitational action for spacetimes with nonsmooth boundaries," *Phys. Rev. D*, vol. 47, pp. 3275–3280, 8 Apr. 1993. DOI: 10.1103/PhysRevD.47.3275. [Online]. Available: https://link.aps.org/doi/10.1103/PhysRevD.47.3275.

[53] D. Brill and G. Hayward, "Is the gravitational action additive?" *Physical Review D*, vol. 50, no. 8, pp. 4914–4919, Oct. 1994. DOI: 10.1103/physrevd.50.4914. [Online]. Available: https://doi.org/10.1103%2Fphysrevd.50.4914.

[54] K. Parattu, S. Chakraborty, B. R. Majhi, and T. Padmanabhan, "A boundary term for the gravitational action with null boundaries," *General Relativity and Gravitation*, vol. 48, no. 7, Jun. 2016. DOI: 10.1007/s10714-016-2093-7. [Online]. Available: https://doi.org/10.1007%2Fs10714-016-2093-7.

[55] L. Lehner, R. C. Myers, E. Poisson, and R. D. Sorkin, "Gravitational action with null boundaries," *Physical Review D*, vol. 94, no. 8, Oct. 2016. DOI: 10.1103/physrevd.94.084046. [Online]. Available: https://doi.org/10.1103%2Fphysrevd.94.084046.

[56] A. Bernamonti, F. Galli, J. Hernandez, R. C. Myers, S.-M. Ruan, and J. Simó n, "Aspects of the first law of complexity," *Journal of Physics A: Mathematical and Theoretical*, vol. 53, no. 29, p. 294 002, Jul. 2020. DOI: 10.1088/1751-8121/ab8e66. [Online]. Available: https://doi.org/10.1088%2F1751-8121%2Fab8e66.